BEST AVAILABLE IMAGES

Defective images within this document are accurate representations of the original documents submitted by the applicant.

Defects in the images may include (but are not limited to):

- BLACK BORDERS
- TEXT CUT OFF AT TOP, BOTTOM OR SIDES
- FADED TEXT
- ILLEGIBLE TEXT
- SKEWED/SLANTED IMAGES
- COLORED PHOTOS
- BLACK OR VERY BLACK AND WHITE DARK PHOTOS
- GRAY SCALE DOCUMENTS

IMAGES ARE BEST AVAILABLE COPY.

As rescanning documents *will not* correct images, please do not report the images to the Image Problem Mailbox.

PCT WORLD INTELLECTUAL PROPERTY ORGANIZATION
International Bureau

INTERNATIONAL APPLICATION PUBLISHED UNDER THE PATENT COOPERATION TREATY (PCT)

(51) International Patent Classification 6 : A61B 5/055 — A1

(11) International Publication Number: **WO 99/55230**

(43) International Publication Date: 4 November 1999 (04.11.99)

(21) International Application Number: PCT/US99/09177

(22) International Filing Date: 27 April 1999 (27.04.99)

(30) Priority Data:
60/083,311 28 April 1998 (28.04.98) US

(71) Applicant *(for all designated States except US)*: HYAL PHARMACEUTICAL CORPORATION [CA/CA]; 2425 Skymark Avenue, Mississauga, Ontario L4W 4Y6 (CA).

(72) Inventors; and

(75) Inventors/Applicants *(for US only)*: KIDD, George, Harrison [US/US]; 3514 North Summit Avenue, Shorewood, WI 53211–2660 (US). MIKULIS, David, John [US/CA]; 40 Byron Street, Oakville, Ontario L6J 7P9 (CA). NAGY, James, I. [CA/CA]; 1662 McCreary Road, Winnipeg, Manitoba R3P 0M7 (CA). TURLEY, Eva, Anne [CA/CA]; Suite 104, 234 St. Clair Avenue West, Toronto, Ontario M4V 1R4 (CA). WINNIK, Francoise, Martine [CA/CA]; 50 Main Street #208, Dundas, Ontario L9H 6P8 (CA).

(74) Agents: DICHTER, Eric, A. et al.; Ratner & Prestia, 301 One Westlakes (Berwyn), P.O. Box 980, Valley Forge, PA 19482–0980 (US).

(81) Designated States: AE, AL, AM, AT, AU, AZ, BA, BB, BG, BR, BY, CA, CH, CN, CU, CZ, DE, DK, EE, ES, FI, GB, GD, GE, GH, GM, HR, HU, ID, IL, IN, IS, JP, KE, KG, KP, KR, KZ, LC, LK, LR, LS, LT, LU, LV, MD, MG, MK, MN, MW, MX, NO, NZ, PL, PT, RO, RU, SD, SE, SG, SI, SK, SL, TJ, TM, TR, TT, UA, UG, US, UZ, VN, YU, ZA, ZW, ARIPO patent (GH, GM, KE, LS, MW, SD, SL, SZ, UG, ZW), Eurasian patent (AM, AZ, BY, KG, KZ, MD, RU, TJ, TM), European patent (AT, BE, CH, CY, DE, DK, ES, FI, FR, GB, GR, IE, IT, LU, MC, NL, PT, SE), OAPI patent (BF, BJ, CF, CG, CI, CM, GA, GN, GW, ML, MR, NE, SN, TD, TG).

Published
With international search report.

(54) Title: HYALURONAN–BASED IMAGING AGENTS

(57) Abstract

Imaging agents containing hyaluronan (HA) and contrast agents. These imaging agents may include HA complexed with gadolinium, optionally with liposomes, and HA complexed with superparamagnetic iron oxides. A method of producing HA–based imaging agents includes mixing a solution of HA with a solution of contrast agent. A method of imaging using HA–based imaging agents includes using HA–based imaging agents to view cancer cells with magnetic resonance.

FOR THE PURPOSES OF INFORMATION ONLY

Codes used to identify States party to the PCT on the front pages of pamphlets publishing international applications under the PCT.

AL	Albania	ES	Spain	LS	Lesotho	SI	Slovenia
AM	Armenia	FI	Finland	LT	Lithuania	SK	Slovakia
AT	Austria	FR	France	LU	Luxembourg	SN	Senegal
AU	Australia	GA	Gabon	LV	Latvia	SZ	Swaziland
AZ	Azerbaijan	GB	United Kingdom	MC	Monaco	TD	Chad
BA	Bosnia and Herzegovina	GE	Georgia	MD	Republic of Moldova	TG	Togo
BB	Barbados	GH	Ghana	MG	Madagascar	TJ	Tajikistan
BE	Belgium	GN	Guinea	MK	The former Yugoslav Republic of Macedonia	TM	Turkmenistan
BF	Burkina Faso	GR	Greece			TR	Turkey
BG	Bulgaria	HU	Hungary	ML	Mali	TT	Trinidad and Tobago
BJ	Benin	IE	Ireland	MN	Mongolia	UA	Ukraine
BR	Brazil	IL	Israel	MR	Mauritania	UG	Uganda
BY	Belarus	IS	Iceland	MW	Malawi	US	United States of America
CA	Canada	IT	Italy	MX	Mexico	UZ	Uzbekistan
CF	Central African Republic	JP	Japan	NE	Niger	VN	Viet Nam
CG	Congo	KE	Kenya	NL	Netherlands	YU	Yugoslavia
CH	Switzerland	KG	Kyrgyzstan	NO	Norway	ZW	Zimbabwe
CI	Côte d'Ivoire	KP	Democratic People's Republic of Korea	NZ	New Zealand		
CM	Cameroon			PL	Poland		
CN	China	KR	Republic of Korea	PT	Portugal		
CU	Cuba	KZ	Kazakstan	RO	Romania		
CZ	Czech Republic	LC	Saint Lucia	RU	Russian Federation		
DE	Germany	LI	Liechtenstein	SD	Sudan		
DK	Denmark	LK	Sri Lanka	SE	Sweden		
EE	Estonia	LR	Liberia	SG	Singapore		

HYALURONAN-BASED IMAGING AGENTS

TECHNICAL FIELD

The present invention relates generally to imaging agents and, more particularly, to Hyaluronan-based imaging agents useful for targeting specific cells.

BACKGROUND OF THE INVENTION

Hyaluronan, also known as Hyaluronic Acid (HA), is a naturally occurring linear polysaccharide consisting of alternating D-glucuronic acid and N-acetyl-D-glucosamine, optionally used as the sodium salt thereof. It is an ancient molecule that is produced by some prokaryotes and almost all eukaryotes. It is sequestered in connective tissue as part of the extracellular matrix and accumulates in large quantities in the vitreous body of the eye and in joints.

Its synthesis is tightly regulated during development and response to injury and its production is enhanced during human tumor progression. When HA is sequestered within the extracellular matrix its primary role appears to be biophysical due to its remarkable viscoelastic properties. Relatively recent studies suggest, however, that HA can also interact specifically and with high affinity ($K_d \approx 10^{-9}$ M) with two receptors, termed CD44 and RHAMM, when these are expressed on cells. CD44 belongs to the link module class of HA binding proteins and RHAMM belongs to a separate protein family. The expression of these two receptors is elevated on some human tumors.

Both CD44 and RHAMM are critically involved in regulating cell motility and proliferation, and both are overexpressed during experimental tumor progression and following response to injury. It has been reported that antibodies to RHAMM and to CD44 inhibit cell motility in response to subculture, injury, and transformation by oncogenes. Overexpression of specific CD44 isoforms enhances metastatic properties of experimental tumors and overexpression of RHAMM is transforming in mice fibroblasts. These effects of CD44 and RHAMM on cell motility and proliferation absolutely require their HA binding capability. CD44 and RHAMM overexpression, not surprisingly, has also been linked to human tumors including myeloma, pancreatic, lung, and breast cancer. The role of overexpression of specific CD44 isoforms in breast cancer and their utility for prognostic indication are unclear, but RHAMM overexpression, particularly within small subsets of cells in the primary tumor and within metastasis is prognostic of poor outcome in two geographically distinct populations. Further, overexpression of RHAMM enhances the prognostic value of commonly used tumor

parameters, including lymph node status and metastasis free survival. Interestingly, the levels of CD44 and RHAMM expression in human tumors are often inversely related, suggesting that these receptors may exert overlapping functions during human neoplasia. There is a need to target CD44 and RHAMM cells and other cells prognostic of tumor presence for imaging, including magnetic resonance imaging.

Magnetic resonance (MR) images are based on the signal from hydrogen nuclei contained in hydrogen-rich compounds in the body: water and lipids. Image contrast depends primarily on two inherent properties of different tissues, specifically the hydrogen content (spin density) and the proton relaxation times (T_1, T_2, and T_2^*). MR contrast agents shorten proton relaxation times of tissues containing them and, therefore, alter the signal intensity on MR images. MR contrast agents are of two types, endogenous and exogenous, the first of which comprises the many forms of endogenous iron, such as ferritin. The second type is represented by small chelate complexes of (typically) gadolinium (Gd^{3+}) ions, and large particulates of coated iron oxides, generally introduced intravenously.

Superparamagnetic materials exhibit extremely large magnetic moments, even in weak external magnetic fields. The large magnetic moments associated with superparamagnetic iron oxide particles in tissues cause local field inhomogeneities which are used to improve detection of lesions by increasing lesion conspicuity in magnetic resonance imaging. The more specific the accumulation of a contrast agent within the target tissue, the better the resulting lesion-tissue contrast. Under ideal conditions, a useful magnetic iron oxide contrast agent should preserve its integrity once injected, escape rapid metabolism, selectively recognize the target, and bind to it. Unfortunately, most colloidal superparamagnetic iron oxides are taken up rapidly by cells of the macrophage monocyte phagocytic system, preventing useful amounts of label from being delivered to specific tissues.

In order to target these contrast agents to specific tissues, it is necessary to incorporate them within a "carrier" system. Typical carriers include proteins, antibodies, polysaccharides, cells, and liposomes.

Amphiphilic molecules, such as surfactants or lipids self-assemble in water forming structures such as micelles, bilayers, tubes or vesicles. Nature provides many examples of such molecules which play key roles in the stability and functions of all cells and organisms. During the past twenty years, chemists have prepared a large number of synthetic amphiphiles, in particular hydrophobically-modified polymers, consisting of a water-soluble polymer onto which a small number of hydrophobic groups are attached by a covalent bond.

Liposomes are vesicles consisting of a lipid bilayer which encloses an aqueous pocket. These aqueous pools can be loaded with water-soluble agents such as drugs or imaging reagents. In addition, liposoluble molecules can be dissolved in the liposome bilayer. Thus, liposomes can be used to carry a broad range of molecules. This property has been exploited in the design of in-vivo drug delivery systems. A recent patent application of Hyal Pharmaceutical Corp. (PCT/GB97/02665, filed September 29, 1997) indicates that hyaluronan-liposome compositions can be formed and used as delivery systems. It is important to recall that the performance of hyaluronan-modified liposomes as drug carriers is directly related to the reliable anchoring of the polymer within the lipid bilayer. One aspect of particular importance is the life span of the lipid/polymer complexes. Some macromolecules with great affinity to the bilayer may in fact be in a fast dynamic equilibrium between the bound and free states. If this is the case, the liposomes will lose their polymer coating very rapidly after injection into the blood stream. Thus, there is a need to address this shortcoming of conventional polymer/liposome systems.

The most widely investigated polysaccharide carrier is arabinogalactan, a naturally occurring polysaccharide which seems to have an affinity for receptors on hepatocytes. Other polysaccharides, such as fucoidan, mannan, and chitosan, have also been studied. Most of these compounds show predominant biodistribution to liver, spleen, kidneys, and lungs.

The preparation and properties of hydrophobically-modified polysaccharides have been investigated and utilized in biotechnology and medicine. This research has focused on polymers such as pullulan, dextran, and mannan partially substituted by various hydrophobic groups, such as long alkyl chains and cholesterol. It has been demonstrated that these polysaccharides effectively coated liposomal surfaces, and rendered the liposomes more stable against external stimuli, such as pH, ionic strength, and in-vivo biodegradation by enzymes and serum proteins, compared with conventional liposomes. Similar effects have been found with liposomes protected with hydrophobically-modified poly-(N-alkylacrylamides).

Paramagnetic metal complexes are exogenous MR contrast agents. Gadolinium is the paramagnetic metal that contains the largest number of unpaired electrons and is, thus, theoretically, the most efficient T_1 relaxation metal that can be used in contrast media for MR imaging. When administered as free Gd^{3+} the metal is extremely toxic. However, when bound to a chelating agent, it loses its toxicity but still maintains its paramagnetic properties. As in the case of superparamagnetic iron oxides, stringent requirements are placed on the Gd^{3+}-chelates for them to become acceptable contrast agents. Aside from standard pharmaceutical features such as water solubility and shelf stability, there are three main general requirements: a) sufficient relaxivity (effici ncy of the proton relaxation enhancement); b) specific in-vivo

distribution; and c) in-vivo stability, excretability, and lack of toxicity. Gd^{3+} image-enhancement products are available commercially. Two such products are those sold under the trademarks, Omniscan® (from Sanofi Winthrop) and Magnevist® (from Berlex Canada Inc.).

A variety of methods have been developed to improve tissue and blood-brain barrier penetration of image enhancement agents. Although significant advances have been made, most such methods have drawbacks or cannot be applied generally. For instance, with many image enhancement agents, uptake of the agents by cells in the liver or elsewhere, prior to reaching their site of delivery has been found.

SUMMARY OF THE INVENTION

To achieve these and other objects, and in view of its purposes, the present invention provides HA-based contrast-enhancing imaging agents for targeting specific cells.

These HA-based contrast agents target specific cells, display sufficient relaxivity, and are otherwise characterized by a specific in vivo distribution, in vivo stability, excretability, and a lack of toxicity.

HA-based contrast agents of this invention are of three types, HA-complexed gadolinium (HA-Gd or Gd-HA), HA-complexed superparamagnetic iron oxides (HA-Fe), and HA-Gd complexed with liposomes (HA-Gd-liposomes).

Gadolinium can be prepared within an HA carrier, yielding an HA-Gd gel, and can also be bonded to complexing agents attached to HA. Liposomes can optionally be incorporated into the HA-Gd combination.

Superparamagnetic iron oxides can be prepared within an HA carrier, yielding an HA-iron oxide nanocomposite which can be isolated as a viscoelastic gel, a ferrofluid, or a dried powder.

In another aspect of the invention, HA-based magnetic resonance (MR) contrast agents are believed to enable HA-receptor-directed imaging of human breast cancer cells by targeting the HA receptors, CD44 and RHAMM.

In another aspect of the present invention, methods of detecting and imaging with breast cancer and other cells using HA-Gd, HA-Fe and HA-Gd-liposomes with Magnetic Resonance (MR) imaging are disclosed.

In another aspect of the present invention, methods of preparing HA-based MR contrast agents are disclosed.

In another aspect of the present invention, methods of determining the smallest size of tumor detectable by HA-based contrast agents in vivo are disclosed.

In another aspect of the present invention, the role of HA-based contrast agents in targeting CD44 and RHAMM in tumor cells is determined. Also, a method of determining whether a tumor cell is benign or malignant is performed by measuring the presence or absence of an HA receptor with an HA-based imaging agent and determining the presence or absence of an HA receptor.

It is to be understood that both the foregoing general description and the following detailed description are exemplary, but are not restrictive, of the invention.

BRIEF DESCRIPTION OF THE DRAWING

The invention is best understood from the following detailed description when read in connection with the accompanying drawing. It is emphasized that, according to common practice, the various features of the drawing are not to scale. On the contrary, the dimensions of the various features are arbitrarily expanded or reduced for clarity. Included in the drawing are the following figures:

FIG. 1 is a table showing the characteristics of human breast cancer cell lines;

FIG. 2 is a scintigraphic image of a nude rat showing the association of radiolabeled HA with a tumor in the rat;

FIG. 3 is a scintigraphic image of a nude rat showing the association of radiolabeled HA with the carotid artery of the rat;

FIG. 4 is a graph showing the molecular weight distribution of hyaluronan after being injected intravenously;

FIG. 5 is a depiction of two reaction schemes whereby HA is linked to a gadolinium complexing agent;

FIG. 6 is a graph showing the effect of pH and concentration of phosphate buffer on the electrophoretic mobility of HA-iron oxide particles;

FIG. 7 is a depiction of the hydrophobically-modified HA complexed with liposomes;

FIG. 8 is a depiction of the pathway for modifying HA by attaching Diethylenetriamine pentaacetic acid (DTPA) and complexing to gadolinium;

FIG. 9 is a graph showing the MRI signal intensity of HA-Gd linked to sepharose beads and free Gd as a function of concentration;

FIG. 10 is a graph showing the signal intensity of HA-Gd and free Gd in the liver as a function of time;

FIG. 11 is a graph showing the signal intensity of HA-Gd and free Gd in skeletal muscle as a function of time;

FIG. 12 is a graph showing the expression of CD44 and RHAMM cell surface receptors in benign and malignant tumor cells using FACS analysis;

FIG. 13 is a graph showing the uptake of Texas red-labeled HA in benign and malignant tumor cells as a function of concentration;

FIG. 14 is a graph showing the uptake (internalization) of labeled HA by different cell lines that express differing levels of HA receptors as a function of time;

FIG. 15 is a graph showing the MRI signal intensity of benign and malignant tumor cells as a function of percentage HA-Gd substitution levels;

FIG. 16 is a depiction of signal intensity at specific tissues within a rat injected with HA-Gd;

FIG. 17 is a graph showing the effect of the anti-CD44 antibody, KM201, on the signal intensity of labeled HA added to different cell lines that express HA receptors; and

FIG. 18 is a depiction of confocal fluorescent images showing the effect of the anti-CD44 antibody, KM201, on the uptake of labeled HA in different cell lines.

DETAILED DESCRIPTION OF THE INVENTION

Hyaluronan (HA)-based magnetic resonance (MR) contrast agents are used to enable HA-receptor-directed imaging of cells. These cells can be tumor cells of different cancers, including breast, colorectal, and lung cancers.

A specific application for an embodiment of the HA-based imaging agents is in the visualization of human breast cancer cells. FIG. 1 shows certain characteristics of specific human breast cancer cell lines. As illustrated by FIGS. 2 and 3, it has been shown in rats that HA injected at a concentration of between 3-10 milligrams/milliliter $(mg\ ml)^{-1}$ retains its high molecular weight for 48 hours, and, thus, is able to bind to the hyaluronan receptors CD44 and RHAMM.

Specifically, FIG. 2 shows the targeting of ^{125}I-HA to a rat colorectal tumor cell line that displays high levels of the HA receptor, CD44. FIG. 3 shows the targeting of ^{125}I-HA to balloon catheter-injured rat carotid arteries, when the site displays maximum levels of the HA receptors, CD44 and RHAMM. Both of the images of FIGS. 2 and 3 were detected using a phosphoimager.

Further, FIG. 4 shows the molecular weight distribution of 6 mg/kg hyaluronan to be greater than 750,000 daltons 24 hours after being injected intravenously. In particular, the graph shows the HA concentration (ng/ml) as a function of elution volume (ml) and molecular weight (kDa). The assay leading to this result was conducted on a B16 Molecular Weight

Calibration Sephacryl 500-HR 1.6x61.5 cm column. HA injected at this concentration retained its high molecular weight, and, thus, it will be able to interact with HA receptors, CD44 and RHAMM.

HA used in the present invention has an average molecular weight of between about 20,000 and about 200,000 Daltons. A more preferred value for the average molecular weight is about 50,000 to about 100,00 Daltons. It is believed that sonication of HA to reduce the average molecular weight to between about 20,000 and about 50,000 would improve penetration of the HA-based imaging agent made from the sonicated HA.

There is reason to believe a similar effect can be demonstrated in humans. Indeed, it also has been shown in rats that ^{125}I-HA specifically deposits at tumors and sites of injury where high levels of these two hyaluronan receptors are expressed. In addition, RHAMM and CD44 are overexpressed during breast cancer progression. Indeed, the presence of subsets of cells within primary breast cancers that overexpress RHAMM is prognostic of poor outcome. To investigate the efficacy of imaging targeted HA, human breast cancer cell lines that express varying levels of RHAMM and CD44 are used and grown as xenographs in nude rats.

Hyaluronan-based contrast agents are of three types, HA-complexed gadolinium (HA-Gd or Gd-HA), HA-complexed superparamagnetic iron oxides (HA-Fe), or HA-Gd complexes with liposomes. The contrast agents are prepared by the synthesis and characterization of polysaccharide-based iron oxides and of complexes of modified HA with gadolinium, optionally with liposomes. To test the use of these as target contrast agents, these contrast agents are administered intravenously. The role of CD44 and RHAMM in targeting HA to breast carcinomas is assessed by attempting to interrupt the binding of HA-Gd (optionally with liposomes) or HA-Fe with either blocking antibodies specific to RHAMM or CD44, or antisense peptides prepared against the HA binding domains of these receptors (see the explanation of FIGS. 17 and 18 below).

Properties of HA and Targeting

The physico-chemical properties of HA, its metabolism, and the consistent demonstration of its upregulation at specific HA cell membrane receptor sites characteristic of disease, injury, and neoplastic transformation demonstrate that HA is an ideal drug carrier and targeting agent for a wide variety of indications and pharmacological agents. In addition, a process has been developed to administer a preloading dose of chondroitin sulfate that binds to the liver scavenger receptor responsible for the uptake of HA by the liver. Using this approach, the amount of HA targeted to the liver can be reduced by over 80%. This treatment does not

alter the ability of HA to target to sites expressing CD44 and RHAMM, because these receptors are molecularly distinct from the scavenger receptors of the liver.

Link between HA Receptors and Malignant Cancer Cells

Increased deposition of HA within both colorectal and breast cancer tumors and the surrounding stroma has recently been linked with poor patient prognosis and tumor invasion/metastasis. Indeed, overexpression of HA receptors (i.e., RHAMM and CD44) is frequently associated with human tumor progression, particularly in breast cancer. HA complexed with gadolinium (HA-Gd) can be used for imaging disease conditions in malignant tumors. Specifically, it can be used to preferentially detect malignant breast cancer cells.

Malignant human breast cancer cells have been shown to express higher levels of HA receptors than benign human tumor cells and to take up labeled HA at much greater rates than benign tumor cells. This uptake has been shown to be specific to HA and to be mediated by HA receptors, such as CD44 and RHAMM. Further, human malignant tumor cells exposed to HA-Gd exhibit a stronger signal intensity in magnetic resonance imaging (MRI) than benign tumor cells, providing in vitro evidence of the effectiveness of HA-Gd in targeting tumor cells. HA-Gd was shown to be rapidly taken up in a dose-dependent manner by the liver, which expresses high levels of HA receptors. The signal intensity of HA-Gd was strongly increased from benign to malignant tumor cells relative to equivalent amounts of free gadolinium, which did not show a dose-dependent increase in signal intensity.

Tissue, such as muscle, which does not express cell surface HA receptors, did not preferentially take-up HA-Gd relative to free gadolinium. The signal intensity was low and it was not increased with increasing amounts of HA-Gd. These results indicate that tissue can be strongly and preferentially imaged with HA-Gd if it expresses HA receptors.

HA-Gd was coupled to agarose beads, washed to remove unbound material, and imaged with MRI compared to an equivalent amount of free gadolinium also coupled to beads and washed to remove unbound material. This test was performed without targeting to any cells. As shown in FIG. 9, the signal intensity of the HA-Gd linked to sepharose beads is significantly higher than that of free gadolinium at a concentration of greater than 1 mg/ml and, in fact, it increases with increasing concentration while free gadolinium remains virtually constant. These results indicate that HA-Gd, unlike the free gadolinium, provides specific receptor binding sites which allows its signal intensity to increase.

HA-Gd administered in increasing concentrations to rats resulted in a dose-dependent signal enhancement in the liver, which contains large amounts of hyaluronan receptors. As

depicted in FIG. 10, free gadolinium (Gd-DPTA at 9.6 mg/kg and Gd-DPTA at 19.2 mg/kg) did not show a similar dose-dependent increase and the signal intensity was always lower than that of HA-Gd even though the Gd-DPTA at 19.2 mg/kg corresponds to the amount of gadolinium complexed within 100 mg/ml of HA-Gd. This demonstrates that uptake of HA is receptor-mediated.

The weight of the HA-Gd is based upon the weight of the hyaluronan and does not reflect the amount of gadolinium that is complexed. In general, the percentage of gadolinium relative to hyaluronan that is attached to the polysaccharide is between about 3.0 and about 12.0%, with a preferred range between about 5.6 and about 9.6%.

FIG. 11 represents the same animal tests as shown in FIG. 10, except that, instead of liver cells, skeletal muscle was measured by MRI. In FIG. 11, signal intensity for HA-Gd uptake was much lower in the skeletal muscle tissue than in the liver. In skeletal muscle, the HA-Gd signal did not change significantly with changes in dose and was more similar to that of free gadolinium. Thus, it appears that skeletal muscle, unlike tumors and liver cells, does not express cell-surface hyaluronan receptors.

Two human breast cancer cell lines, one of which has been previously characterized as malignant (MDA-MM-231) and one of which has been previously characterized as benign (MCF-7) when grown as xenografts in nude mice, were analyzed for the expression of the cell surface hyaluronan receptors, RHAMM (black) and CD44 (white), using FACS analysis. FIG. 12 shows that the malignant tumor cells (MDA-MM-231) express much higher levels of these receptors in vitro than the benign tumor cells (MCF-7), thus demonstrating the importance of these receptors in imaging and treatment of malignant cells.

Texas red-labeled hyaluronan was added to the above two malignant and benign cell lines in vitro to assess whether or not the labeled HA would be taken up differentially by the cell lines. As can be seen in FIG. 13, both cell types showed an increase in uptake of the labeled hyaluronan with increasing concentrations and both cell types showed a plateau of this uptake. These results are consistent with the position that uptake is receptor-mediated. Because the malignant tumor cells took up approximately 2.5 fold more labeled HA than the benign tumor cells, it appears that malignant tumors take up HA-Gd better than benign tumors.

To assess how long cells must be exposed to labeled HA for uptake to occur and to further assess the role of RHAMM and CD44 in the uptake process, several additional cell lines were examined. 10T1/2 fibroblasts (10T) were transfected with RHAMM/CD44 (LR21). Mutant active ras (c3) which highly express RHAMM and CD44 were compared to malignant (MDA) and benign (MCF) cells. Fluorescent dextran was used as a background control to

assess the specificity of HA uptake. The results, which are depicted in FIG. 14, clearly demonstrate that cells which overexpress RHAMM or CD44 receptors (i.e., MCF and c3 cell lines) show specifically enhanced uptake of Texas red-labeled HA.

Pellets of benign and malignant human breast tumor cells were exposed to HA-Gd of differing percentage Gd substitution levels, they were then washed, and, finally, they were suspended within collagen gels. Then, signal intensity from MRI was determined. As shown in FIG. 15, the malignant (invasive, MDA-MB-231) tumor cells exhibited a higher signal intensity than the benign tumor cells (non-invasive, MCF-7) at a range of Gd concentrations (0.5, 2, and 10 mg/ml). The signal was maximized with a Gd-HA (labeled Gd) preparation of 9.4-9.6% Gd substitution levels. These results indicate that it is possible to differentially image benign versus malignant human tumor cells using Gd-HA in vitro.

Malignant breast cancer cells (MDA-MB-231 cells) were grown as xenografts in nude rats and the animals were injected with 100 mg/kg of Gd-HA (HA, 5.6% complexed, represented as "B"). The control was the nude rat before exposure to Gd-HA (represented as "A"). As shown in FIG. 16, there is increased signal intensity within the tumor (its location indicated by the arrow in FIG. 16) and in liver cells. These results indicate a high probability of imaging malignant tumors in vivo with HA-Gd imaging agents.

As shown in FIG. 17, when an anti-CD44 antibody, KM201, is added to 10T1/2 (low receptor expression) and LR21 (high receptor expression/RHAMM transfected) cell lines, the uptake of Texas red-labeled HA (200 mg/ml) by the cell lines is significantly decreased versus Texas red-labeled HA in the absence of antibody. Similar results are shown in the confocal fluorescent images of FIG. 18. Specifically, when 50 μm/ml of the anti-CD44 antibody, KM201, is added to 10T1/2 parenteral and RHAMM transfected (LR21) cell lines, the uptake of Texas red-labeled HA by the cell lines is significantly decreased versus Texas red-labeled HA in the absence of antibody, i.e., higher resolution in the unblocked images.

Further studies have shown that colocalization of RHAMM receptors and erk molecules occurs in the nucleus of MDA-MB-231 (malignant) cells, but is perinuclear in MCF-7 (benign) cells. In addition, overexpression of ras molecules correlates with overexpression of erk molecules and RHAMM receptors in breast cancer cells. Also, RHAMM expression correlates with ras proto-oncogene or mutant active ras expression in MCF-10A cells. Finally, RHAMM overexpression correlates with overexpression of active erk1, ras, and CD44.

Preparation, chemical and physical characterization of HA-stabilized MR contrast agents

Ferrofluids/Iron Oxides

Preparing HA-stabilized ferrofluids involves the preparation of superparamagnetic, nanosized iron oxides within the framework of HA-hydrogels and subsequent conversion of the gels into HA-stabilized ferrofluids. Reaction temperature, pH, and the nature of the oxidant can all affect the Fe^{2+} oxidation in the HA matrix and their effect is determined. The composites are characterized by elemental analysis (Fe content), powder X-Ray crystallography, transmission electron microscopy (TEM) and SQUID magnetometry. The ferrofluids obtained from the magnetic gels are characterized by capillary electrophoresis, dynamic light scattering, and TEM.

Another way of making HA-stabilized MR iron oxides consists of preparing nanosized magnetite in the absence of any surfactant or polymer. The magnetite obtained by this route is stabilized subsequently in physiological media by controlled adsorption of HA. The colloidal stability of the ferrofluids is monitored as a function of polymer concentration using various techniques, including turbidity measurements.

In a preferred method of making HA-iron oxides, a solution of ferric chloride hexahydrate (1.0 g) and ferrous chloride tetrahydrate (0.5 g) in water (200 ml) is purged with nitrogen for 15 minutes. An aqueous solution of NH_4OH (5% by weight) is added to the vigorously stirred solution to raise the pH to 8.0. The mixture is stirred for an additional 15 minutes at the end of the addition. The magnetite obtained can be separated by decantation in the presence of a magnetic field. The magnetite is washed with water until the pH of the supernatant is between about 6 and about 7. The magnetite is then suspended in deionized water to form a stock solution (30 mg/ml). The size of the magnetite particles is 15 nm $\pm$ 3 nm, as determined by transmission electron microscopy (TEM).

An aliquot of the magnetite stock solution (1.0 ml) is added to a solution of HA-NH_2 (its preparation is described below, 0.08 g) in water (5.0 ml). The resulting suspension is treated by sonication using a Microson Ultrasonic Cell Disruptor (2 minutes at power setting 15). The reselecting fluid is washed with a phosphate buffered saline (PBS) buffer (pH 7.33) and purified by elution through a magnetic column. The resulting fluid is treated first with aqueous NaOH (0.1 M) to adjust the pH to 11, then with HCl (0.1 N) to bring the pH to 7.3. The fluid is then filtered through a 0.45 μm filter. Finally, a solution of NaN_3 in water is added to the ferrofluid (final NaN_3 concentration: 10^{-3} M).

Gd Complexes

In preparing HA-based gadolinium contrast agents, several approaches are taken:

(1) Direct binding of Gd^{3+} by HA. Important factors in this process are the binding constant of Gd^{3+} to HA and the selectivity of HA for gadolinium in the presence of other di- and trivalent cations, such as zinc, iron, magnesium, and calcium.

(2) Binding of Gd^{3+} to a complexing agent covalently linked to HA. FIG. 5 shows two possible routes for modifying HA by covalently linking to its backbone a compound which complexes with Gd^{3+}. In Route A, an amine in which the primary amino group is linked to one of three possible Gd^{3+} complexing agents (1, 2 or 3 in FIG. 5) is attached to HA which contains a carboxyl group.

Alternatively, in Route B, a primary amine may be introduced to the HA backbone and then reacted subsequently with macrocycles bearing carboxylic groups. The modified polymers are then treated with gadolinium which will form complexes with the functional groups attached to HA. The resulting modified polymers are characterized by standard chemical means and the binding constant of Gd^{3+} to the polymeric chelating agents is measured. These polymers are then evaluated as MR contrast agents. There are three main factors to consider for making a complex of gadolinium which will be stable in vivo: a) the thermodynamic stability constant of the metal/ligand complex under physiological conditions, b) the selectivity of the ligand for gadolinium, and c) the reaction kinetics.

To assay for the effect of gadolinium and iron chelates on hyaluronan biological activity, the ferrofluids and gadolinium complexes are digested with testicular hyaluronidase. The toxicity of the HA-based contrast agents is measured to determine the extent of complexation.

HA-Gd-liposome systems

In these imaging contrast agents, the gadolinium complex is encapsulated in the inner aqueous pool of the liposome. Hydrophobically-modified HA (HM-HA) 2, as shown in FIG. 7, in which the main chain of HA is partially substituted with hydrophobic groups, is anchored on the outer surface of the phospholipid bilayer 4. These hydrophobic substituents can be inserted into the liposome bilayer, thus providing strong anchoring points 6 for the HA on the external membrane (liposome bilayer).

Liposomes can be prepared by a variety of methods yielding either unilamellar or multilamellar vesicles of narrow size distribution ranging in diameter from 50 nm to 1,000 nm. The liposomes can be obtained first in the absence of HM-HA 2 which can be anchored within the liposome membranes by incubation of "naked" liposome aqueous suspensions in the

presence of HM-HA 2. Surface saturation and stability of the complexes can be determined by techniques including fluorescence spectroscopy, centrifugation, electron microscopy, and gel permeation chromatography. Drugs or imaging agents can be incorporated in the liposomes prior to stabilization with HM-HA 2.

The outer layer of HA serves as a targeting compound for the liposome. Encapsulated materials can be chosen among any known imaging agent, such as for example, the commercial MR imaging agent Magnevist®, or the HA-iron oxide described above, the commercial MR imaging agent Magnevist® along with HA-Gd or any HA-Gd complexing agent described above. The HM-HA 2 is prepared by covalent attachment of hydrophobic groups, such as n-alkyl chains of from about 10 to about 24 carbons or the cholesteryl group. It also may be prepared by activation of the carboxylic acid groups and subsequent conversion to amides and conversion of primary hydroxyls to ethers. Optionally, a fluorescent group such as pyrene or naphthalene can be linked to HA to serve as a probe of the effective anchoring of the HM-HA 2 onto the liposome membrane.

Alternatively, HA may be anchored onto the outer membrane of the liposomes through a crosslinking agent. The crosslinking agent may admixed in the liposomes before they are coated with HA, as discussed in U.S. Patent No. 5,603,872 to Margalit.

The structure of the HM-HA 2 is as follows:

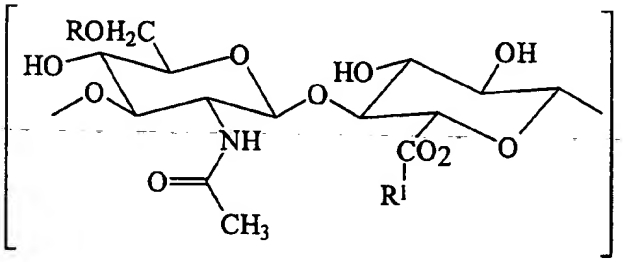

wherein R is $(CH_2)_nCH_3$, 3-cholesteryl, or H and R1 is $X(CH_2)_nCH_3$, $-NHC_6H_{12}NH-$COO(cholesteryl), H, or Na^+.

In addition, the binding of the HM-HA 2 to liposomes can generally be obtained in two steps: (a) preparation of uncoated "naked" liposomes, and (b) incubation of the liposome suspension in the presence of HM-HA. Binding can be measured by fluorescence spectroscopy, gel permeation chromatography, and centrifugation assays. The physico-chemical stability of HM-HA coated liposomes against external stimuli, such as pH, ionic strength, and in vitro degradation by serum protein, and surface saturation can also be evaluated using the assays used to measure binding. It is believed that MR contrast agents, such as gadolinium, are

encapsulated in the modified liposomes, either in the aqueous core of the liposomes or within the lipid bilayer. The resulting materials can then be tested following the protocols employed in the evaluation of the other HA-based contrast agents.

Binding of gadolinium to complexing agents attached to HA

In a group of experiments, whose reaction schemes are depicted in FIG. 5, HA has been modified with ethylene diamine, hydrazine monohydrate, and diethylenetriamine (as described below), where the complexing agent is linked to a small amount of the HA carboxylic groups. Alternatively, the complexing agent is linked to the C6 position of the HA disaccharide units. The final gadolinium-HA complexes are analyzed by all of the methods described above.

Modification of HA with Ethylenediamine

Ethylenediamine (1.2 g, 20 mmol) was added to a solution of sodium hyaluronan (200 mg, 0.50 mmol) in water (50 ml). The pH of the reaction mixture was adjusted to 4.75 using 0.1 N HCl. Then, 1-ethyl-3-(3-dimethylaminopropyl) carbodiimide (EDC, 382 mg, 2.0 mmol) was added in solid form. The pH of the reaction mixture was maintained at 4.75 by addition of 0.1 N HCl and the mixture was stirred at room temperature for 12 hours. After this period, the pH of the reaction mixture was adjusted to 7.0 by addition of 1 N NaOH. The mixture was subjected to ultrafiltration using a YM30 membrane. The resulting viscous polymer solution was diluted with water. This aqueous polymer solution was added into a large amount of methanol. The solid precipitated polymer was separated by vacuum filtration, washed with methanol, redissolved in the minimum amount of water, and lyophilized for 24 hours to obtain a yield of 350 mg of the ethylenediamine-modified HA.

Modification of HA with Diethylenetriamine

Diethylenetriamine (2.06 g, 20 mmol) was added to a solution of sodium hyaluronan (200 mg, 0.50 mmol) in water (50 ml). The pH of the reaction mixture was adjusted to 4.75 using 0.1 N HCl. Then, 1-ethyl-3-(3-dimethylaminopropyl) carbodiimide (EDC, 382 mg, 2.0 mmol) was added in solid form. The pH of the reaction mixture was maintained at 4.75 by addition of 0.1 N HCl and the mixture was stirred at room temperature for 12 hours. After this period, the pH of the reaction mixture was adjusted to 7.0 by addition of 1 N NaOH. The mixture was subjected to ultrafiltration using a YM30 membrane. The resulting viscous polymer solution was diluted with water and subjected to a second ultrafiltration. The resulting concentrated aqueous polymer solution was lyophilized for 24 hours to obtain a yield of 340 mg of the diethylenetriamine-modified HA.

Modification of HA with Hydrazine Monohydrate

Hydrazine monohydrate (1.0 g, 20 mmol) was added to a solution of sodium hyaluronan (200 mg, 0.50 mmol) in water (50 ml). The pH of the reaction mixture was adjusted to 4.75 using 0.1 N HCl. Then 1-ethyl-3-(3-dimethylaminopropyl) carbodiimide (EDC, 382 mg, 2.0 mmol) was added in solid form. The pH of the reaction mixture was maintained at 4.75 by addition of 0.1 N HCl and the mixture was stirred at room temperature for 12 hours. After this period, the pH of the reaction mixture was adjusted to 7.0 by addition of 1 N NaOH. The solution was transferred to a dialysis bag (molecular weight cutoff: 10,000) and dialyzed exhaustively against water. The resulting aqueous polymer solution was lyophilized for 24 hours to obtain a yield of 300 mg of the hydrazine monohydrate-modified HA.

Modification of HA with Diethylenetriamine pentaacetic acid (DTPA)

Sodium hyaluronate (200 mg, 0.50 mmol) was dissolved in 20 ml of water. The pH of the solution was adjusted to between 3.5 and 4.5 with aqueous hydrochloric acid (0.1 N) and aqueous sodium hydroxide (0.1 N). To this solution, EDC (93 mg, 0.50 mmol) was added, and the pH of the solution was adjusted to between 3.5 and 4.5. Diethylenetriamine pentaacetic acid (DTPA) (38.2 mg, 0.1 mmol) was dissolved in 20 ml of water. The pH of the solution was then adjusted to between 3.5 and 4.5. To this solution, EDC (3.7 mg, 0.02 mmol) was added. The two solutions were mixed together. Ethylenediamine (10 mg, 0.17 mmol) was introduced, and the pH was adjusted again to between 3.5 and 4.5. The reaction mixture was kept at room temperature for 2 hours. Aqueous hydrochloric acid (10 ml, 0.1 M) was added to destroy excess EDC, then the pH was adjusted to 7 with aqueous NaOH (1 M). The mixture was subjected to ultrafiltration using a YM30 membrane. The resulting viscous polymer solution was diluted with water and subjected to a second ultrafiltration. The resulting concentrated aqueous polymer solution was lyophilized for 24 hours to obtain a yield of 240 mg of product.

The three types of modified HA were obtained with yields between 300 and 350 mg, and after modification, they were complexed to gadolinium. Typically, an aqueous solution of modified HA (5 ml, 10 g/L) was added dropwise to a stirred aqueous solution of gadolinium chloride (1 ml, 0.05 to 0.2 M). The mixture was kept at room temperature for 2 hours. It was then transferred in a dialysis bag (12,000 dalton molecular weight cutoff) and dialyzed against water until no Gd^{3+} was detected in the dialyzate, as determined by a colorimetric test using xylenol orange as an indicator. The HA-Gd complex was isolated by lyophilization of the purified solution and a colorless material was obtained. It was then dissolved in physiological buffer to prepare a MR contrast agent solution of concentration from 0.5 to 1.0 g/L. From

observing the modified HA-Gd^{3+} complexes, it appears that these modifications to the C6 position of HA increase the binding affinity for the complexed gadolinium. This results in a more stable complex of HA and gadolinium.

Procedure for the Preparation of DTPA-modified Hyaluronic Acid Complexed with Gadolinium

A pathway for modifying HA by attachment of DTPA is shown in FIG. 8. The sodium salt of HA is shown with two different pathways for its modification, one with Diethylenetriamine pentaacetic acid (DTPA).

The DTPA pathway proceeds with NH_2 groups being attached to the HA with ethylenediamine (EDA) and forming several different preparations, some having different ratios of EDA to NH_2 groups, as shown. The DTPA is then attached to the NH_2 groups on the HA preparations. Finally, the gadolinium is complexed with these preparations to yield HA-Gd-DTPA complexes.

Table 2 shows the water content, determined by gravimetric determination, DTPA molar percentage, obtained from ^1H NMR spectroscopy, and gadolinium content from ICP analysis of the different preparations formed by the pathway described. Table 3 shows the reagent components used in the different preparations. Specifically, it depicts the amount of HA-COONa, DTPA, DCC (1,3-Dicyclohexylcarbodiimide), NHS (N-Hydroxysuccinimide), EEDQ (2-ethoxy-1-ethoxycarbonyl-1,2-dihydroquinoline), and EDA. Table 4 shows the retention times of the different preparations on a column in which retention time is a function of the molecular weight of the preparation.

Table 2: Summary of Physical Properties of HA-DTPA-Gd

Preparation	1:1:10	2:1:10	2:1:50	2:1:50e
water content (wt%)	–	7.04	11.08	7.62
Mol% of DTPA (NMR)	3%	6%	4.2	14.2
Gd content (ICP)	2.05	6.1	1.88	5.17

Table 3: Amounts of Reagents used for HA-DTPA-Gd Preparation

	1:1:10	2:1:10	2:1:50	2:1:50e
HA-COONa	1.00g(2.4x 10^{-3}mol)	1.00g(2.4x 10^{-3}mol)	1.00g(2.4x 10^{-3}mol)	2.00g(4.8x 10^{-3}mol)
EDA	1.63ml(2.4x 10^{-3}mol)	1.63ml(2.4x 10^{-3}mol)	8.14ml(0.121 mol)	16.3ml(0.242 mol)
EEDQ	1.24g(4.9x 10^{-3}mol)	1.24g(4.9x 10^{-3}mol)	1.24g(4.9x 10^{-3}mol)	15.4g(0.0622mol)
DTPA	0.941g(2.4x 10^{-3}mol)	1.91g(4.9x 10^{-3}mol)	1.91g(4.9x 10^{-3}mol)	3.82g(9.8x 10^{-3}mol)
DCC	0.743g(3.6x 10^{-3}mol)	1.511g(7.3x 10^{-3}mol)	1.511g(7.3x 10^{-3}mol)	3.02g(1.46x 10^{-3}mol)
NHS	0.414g(3.6x 10^{-3}mol)	0.845g(7.3x 10^{-3}mol)	0.845g(7.3x 10^{-3}mol)	1.69g(1.46x 10^{-3}mol)

Table 4: Retention Times (minutes) for HA and HA derivatives

	HA	1:1:10	2:1:10	2:1:50	2:1:50e
Peak 1	16.183 major	16.833	16.867	16.167	17.450
Peak 2	27.450 minor	26.283	26.283	26.283	26.317
Peak 3	--	--	31.150	31.167	31.217

Reagents and Materials Used

The reagents used in the DTPA pathway were: Hyaluronic acid (sodium salt), TEAT (1,4,8,11 - Tetraazacyclotetradecane-1,4,8,11-tetraacetic acid tetrahydrochloride tetrahydrate), DTPA (Diethylenetriamine pentaacetic acid), DCC (1,3-Dicyclohexylcarbodiimide), N-Hydroxysuccinimide, EEDQ (2-ethoxy-1-ethoxycarbonyl-1,2-dihydroquinoline), Gadolinium (III) Chloride hexahydrate, Arsenazo III ([2,2'-(1-8-dihydroxy-3,6-disulfonaphthylene-2,7-bisazo)-bisbenzene arsonic acid]), acetonitrile, methanol, ethylenediamine, triethylamine, HCl, and NaOH. Spectra/Por® Molecularporous Dialysis tubing (from Spectrum®) (molecular weight cutoff: 12-14,000) was used also. All water used was purified using a Nanopure deionizing system.

Synthesis of HA-DTPA

(Synthesis of 2:1:10 described below. For amounts of reagents used for other polymers, refer to Table 3)

Attachment of NH_2 groups to HA proceeds as follows:

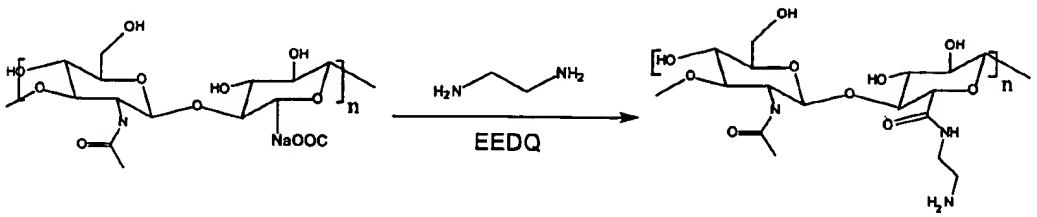

HA-COONa (250 mg, 0.62 mmol COONa) was dissolved in distilled, deionized H_2O (20 ml). The pH (measured with pH paper) was adjusted to 3 with 1.0N HCl. EEDQ (0.309 g, 1.25 mmol) in MeOH (15 ml) was added dropwise to the HA mixture. Ethylenediamine (0.42 ml, 6.2 mol) was added and the mixture was stirred at room temperature for 24 hours.

The mixture was dialyzed against 2L MeOH/H_2O (1:1, v:v) for 3 days, then against 2L H_2O for 3 days (MWCO: 12-14,000 Da). The dialyzed mixture was filtered by vacuum filtration using a sintered glass filter and lyophilized to yield a light, white solid (150 mg, 60% yield).

Attachment of DTPA to HA-NH_2 proceeds as follows:

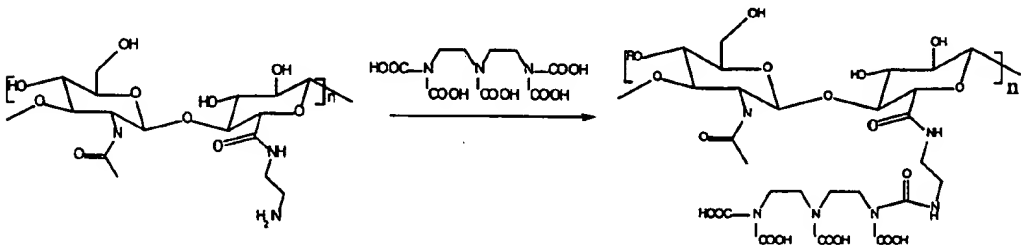

DTPA (0.5 g, 1.26 mmol) in acetonitrile (5 ml) and triethylamine (0.88 , 5X molar amount of DTPA) were stirred at 55°C, until all DTPA was dissolved. After cooling to room temperature, DCC (0.372 g, 1.8 mmol) and N-Hydroxysuccinimide (0.208 g, 1.8 mmol) were added. This mixture was stirred overnight at room temperature.

In a separate round bottom flask, HA-NH_2 (250mg, 0.62mmol NH_2, assuming all COONa groups were aminated) was dissolved in H_2O (20ml) and the pH was adjusted to 10 with 1.0 N NaOH.

The precipitate from the DTPA/acetonitrile mixture was removed by vacuum filtration, and the filtrate was added to the HA-NH_2 solution. The mixture was stirred overnight at room temperature. This mixture was then rotovaporated to remove the solvents, and the resulting gel was redissolved in H_2O, filtered and dialyzed against 2L H_2O for 3 days. The mixture was then acidified (pH 3) and subjected to three consecutive ultrafiltrations using a YM30 membrane (Amicon). The mixture was lyophilized to yield a light, white solid (160mg, 64%yield).

Complexing Gd^{3+} with HA-DTPA proceeds as follows:

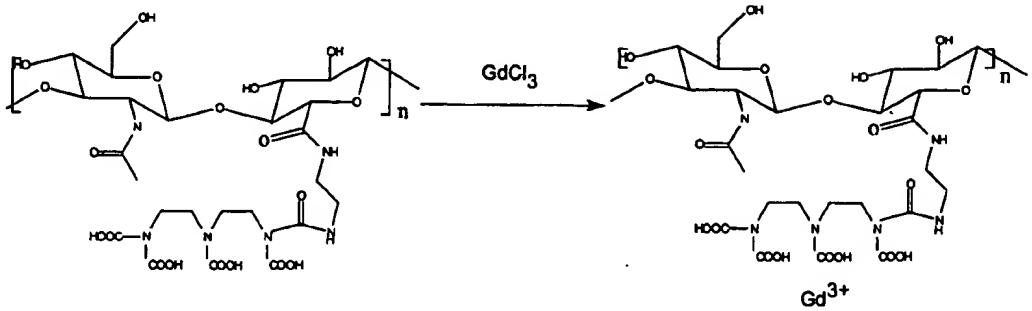

A 1% HA-DTPA solution in H_2O was prepared. To this solution, a 0.1 M $GdCl_3$ solution was added dropwise, and this mixture was subjected to ultrafiltration using a YM30 membrane. $GdCl_3$ was added until the filtrate contained detectable amounts of Gd^{3+}, as detected by a colorimetric test using Arsenazo III in acetate buffer, pH 3.89 at 0.1 ionic strength (NaCl).

The solution was subjected to two additional ultrafiltrations, adding 20ml of H_2O after each filtration cycle. The HA-DTPA-Gd was lyophilized, yielding a light, white solid.

Preparation HA-DTPA-Gd polymer (2:1:50e) had the highest EEDQ, DTPA, and EDA ratios to COOH and gave the highest Gd content. Preparation HA-DTPA-Gd (1:1:10) had the lowest DTPA to COOH ratio and the lowest Gd content (Table 2).

GPC studies, in which preparations were placed on a linear hydrogel column (from Waters) to measure the molecular weight of the preparations, revealed that the molecular weight of HA did not change significantly after modification (see Table 4). The column features cause the retention time on the column to increase as the molecular weight of the preparation tested decreases. The HA did not seem to have degraded under the reaction conditions used.

Preferred Methods of Preparation of Modified HA and Gd

Among the methods of modifying HA for complexing it to Gd are modification with ethylenediamine or with hydrazine. Preferred methods for use of the two modification schemes are described below.

Use of Ethylenediamine

Methods for Attachment of NH_2 to HA with Ethylenediamine

1(a) HA-COONa (1.0 g) was dissolved in distilled deionized water (80 ml). The pH of the solution was adjusted to 3.0 using hydrochloric acid (HCl, 1.0 N). A solution of EEDQ (7.7 g) in methanol (150 ml) was added dropwise to the reaction mixture. The mixture was stirred at room temperature until it turned clear. Ethylenediamine (EDA) was then added to the

reaction mixture, which was stirred at room temperature for 24 hours. The solution was placed in dialysis bags (SpectraPore membrane with a molecular weight cut off (MWCO) of 6,000 to 8,000 Daltons). The solution was dialyzed against methanol/water (1/1 v/v (volume ratio), 2.0 L) for 3 days and against water (2 L) for 3 days. The resulting solution was concentrated by ultrafiltration. The polymer was isolated by freeze-drying (HA-NH_2, 0.3 g)

2(a) HA-COONa (1.0 g) was dissolved in distilled deionized water (80 ml). The pH of the solution was adjusted to 3.0 using hydrochloric acid (HCl, 1.0 N). A solution of EEDO (7.7 g) in dimethylformamide (150 ml) was added dropwise to the reaction mixture. The mixture was stirred at room temperature until it turned clear. Ethylenediamine (EDA, 8 ml) was then added to the reaction mixture, which was stirred at room temperature for 24 hours. The solution was placed in dialysis bags (SpectraPore membrane with a MWCO of 6,000 to 8,000 Daltons). The solution was dialyzed against isopropanol/water (1/1 v/v, 2.0 L) for one day and against water (2 L) for 3 days. The resulting solution was concentrated by ultrafiltration. The polymer was isolated by freeze-drying (HA-NH_2, 0.46 g).

3(a) HA-COONa (2.0 g) was dissolved in distilled deionized water (2000 ml). The pH of the solution was adjusted to 3.0 using hydrochloric acid (HCl, 1.0 N). A solution of EEDQ (15.4 g) in dimethylformamide (150 ml) was added dropwise to the reaction mixture. The mixture was stirred at room temperature until it turned clear. Ethylenediamine (EDA, 18 ml) was then added to the reaction mixture, which was stirred at room temperature for 24 hours. The solution was placed in dialysis bags (SpectraPore membrane with a MWCO of 6,000 to 8,000 Daltons). The solution was dialyzed against isopropanol/water (1/1 v/v, 2.0 L) for one day and against water (2 L) for 3 days. The resulting solution was concentrated by ultrafiltration. The polymer was isolated by freeze-drying (HA-NH_2, 0.96 g).

Methods for Reaction of DTPA to HA-NH_2

1(b) A suspension of DTPA (1.92 g) in acetonitrile (20 ml) was heated to 55°C in the presence of triethylamine (3.4 ml) until complete dissolution. N-Hydroxysuccinimide (0.85 g) and DCC (1.51 g) were added to the cooled solution. The resulting suspension was stirred for 24 hours at room temperature. It was filtered to remove the white precipitate formed. The filtrate was added to a solution of HA-NH_2 (0.5 g, from step l(a)) in water kept at pH 10 by dropwise addition of aqueous sodium hydroxide (1.0 N). The reaction mixture was stirred at room temperature for 24 hours. The mixture was filtered and the filtrate was concentrated by ultrafiltration with exhaustive washes with water. The polymer (HA-DTPA) was isolated by freeze-drying (0.24 g).

2(b) A suspension of DTPA (2.0 g) in acetonitrile (20 ml) was heated to 55°C in the presence of triethylamine (3.4 ml) until complete dissolution. N-Hydroxysuccinimide (0.9 g) and DCC (1.50 g) were added to the cooled solution. The resulting suspension was stirred for 24 hours at room temperature. It was filtered to remove the white precipitate formed. The filtrate was added to a solution of HA-NH_2 (0.5 g, from step 3(a)) in water kept at pH 10 by dropwise addition of aqueous sodium hydroxide (1.0 N). The reaction mixture was stirred at room temperature for 24 hours. The mixture was filtered and the filtrate was concentrated by ultrafiltration with exhaustive washes with water. The polymer (HA-DTPA) was isolated by freeze-drying (1.0 g).

Complexation of HA-DTPA with Gd(III)

A solution of $GdCl_3$ in water (0.1 M) was added to a solution of HA-DTPA in water (1.0% w/w). Excess Gd(III) was removed by ultafiltration with extensive washes with water. The polymer (HA-DTPA-Gd) was recovered by freeze-drying. The Gd content was determined by neutron activation using standard $GdCl_3$ to calibrate the measurement.

Preparation a: Gd content 3.5 wt %, 0.59 g HA-Gd

Preparation b: Gd content 9.4 wt %, 0.71 g HA-Gd

Preparation c: Gd content 9.2 wt %, 1.0 g HA-Gd

Use of Hydrazine

Attachment of Hydrazine to HA

A solution of 1-(3-dimethylaminopropyl)-3-ethylcarboxidiimide (DEC, 1.0 g) in water (25 ml) was added to a solution of HA-COONa (1.0 g) in distilled deionized water (50 ml). The pH of the solution was adjusted to 3.2 using hydrochloric acid (HCl, 1.0 N). The mixture was stirred at room temperature until it turned clear. A solution of adipic dihydrazine (ADH, 4.1 g) in water (50 ml) was then added to the reaction mixture, which was stirred at room temperature for 24 hours. The resulting solution was concentrated by ultrafiltration. The polymer was isolated by freeze-drying (0.6 g HA-ADH).

Attachment of DTPA to HA-ADH

DEC (1.0 g) and DTPA (1.8 g) were added to a solution of HA-ADH (0.6 g) in water (100 ml) and the pH of the mixture was adjusted to 3 with NaOH (0.1 N). The mixture was stirred at room temperature for 24 hours. It was purified by ultrafiltration. The polymer (HA-DTPA) was isolated by freeze-drying (0.59 g).

Complexation of HA-DTPA with Gd(III)

A solution of $GdCl_3$ in water (0.1 M) was added to a solution of HA-DTPA in water (1.0% w/w). Excess Gd(III) was removed by ultrafiltration with extensive washes with water. The polymer (HA-DTPA-Gd) was recovered by freeze-drying (0.52 g; Gd content: 3.5% wt).

Iron Oxide-based Imaging Agents

Superparamagnetic forms of iron oxides are readily prepared within ionic polysaccharides and they can be complexed with HA to obtain an imaging agent. The resulting nanocomposites can be degraded into stable aqueous ferrofluids. HA is used as a template for the preparation of magnetic nanocomposites, and subsequent ferrofluid formation. The crosslinking ion (Fe^{2+}) serves as the reaction center for the in-situ formation of nanocrystalline iron oxides. The oxidation of the ferrous ion leads predominantly to the formation of a superparamagnetic form of iron oxides, either maghemite (γ-Fe_2O_3) or magnetite (Fe_3O_4). The room temperature saturation magnetization of dehydrated gels was 12 emu g^{-1} at 30 kOe for dry specimens containing 21% (w/w) of Fe. These gels were converted into strongly magnetic, colloidally stable ferrofluids by sonication in water or treatment with L-ascorbic acid. Transmission electron microscopy (TEM) analysis of the ferrofluids reveals submicron, crystalline iron oxide particles, 25 to 40 mm in size. The electron diffraction pattern of these particles showed diffraction rings characteristic of γ-Fe_2O_3 and Fe_3O_4. It was difficult to distinguish between the two phases.

Size distribution analysis of ferrofluids by quasi-elastic light scattering (QELS) revealed the presence of three particle distributions. One of the particle distributions detected was in the size range of 20-50 nm. Because the QELS measurements yield the size distribution of the iron oxide particles stabilized by residual chains of HA, a slightly larger size, compared to the TEM results, is expected to account for the corona of polymeric chains surrounding the oxide particles. The histogram also reveals larger particles having a size range of 125-250 nm. This may represent agglomerates of the smaller particles. A further signal centered at 4 nm is attributed to free HA.

The surface charge properties of the ferrofluids were determined by capillary electrophoresis. The HA-iron oxide particles (ferrofluids) elute as a broad band after caffeine used as a neutral marker, indicating that this ferrofluid consists of negatively charged particles. The negative charge is attributed to the carboxylate groups present in the HA chains stabilizing the iron oxide particles. Electrophoretic mobilities and zeta potentials for particles were calculated from the electropherogram. To study the influence of pH, ionic strength and applied

voltage on the surface properties of the particles in the ferrofluid, experiments were conducted by varying the pH, applied voltage, and ionic strength. Results of these experiments indicate that pH and applied voltage do not have any significant effect on electrophoretic mobility within the ranges studied. The electrophoretic mobility is close to 3 x 10^{-8} $m^2/V.sec$ (zeta potential = - 40 mV) for all samples for 10 and 25 mM phosphate buffers, pH 6 to 11 at applied voltages of 15, 20, and 25 kV. Nevertheless, when the buffer concentration is decreased, the electrophoretic mobility increases (see FIG. 6). At higher buffer concentrations, the surface charge on the particles decreases because an increase in Na^+ and PO_4^{3-} ions compresses the electrical double layer surrounding the particle and shields the negatively charged groups on the particle surface.

To prepare nanocomposites, a 10 gram/liter solution of HA was prepared in a 0.1 M solution of $FeCl_2$ in methanol/water (50/50 v/v). Gelation occurred immediately, resulting in the formation of large, clear yellow, hydrogel fragments in the $FeCl_2$ solution. This suspension was kept under a static nitrogen atmosphere at room temperature for 3 hours. Subsequently, the HA gel fragments were thoroughly washed with methanol/water (50/50 v/v) to remove any uncomplexed Fe^{2+} ions from the gel. A 0.5 M solution of NaOH in methanol/water (50/50 v/v) was added to the washed gel to hydrolyze the complexed Fe^{2+} ions. Nitrogen gas was bubbled through this solution for 2 hours. This was followed by 2 hours of oxygen bubbling, resulting in the formation of a brown-colored gel. The reaction cycle (loading) was repeated five times with the same gel batch. The HA gel became darker in color and more magnetic after each loading and oxidation, resulting in a dark brown gel after 5 loading cycles. Freeze dried samples of this nanocomposite gel were used for magnetic property measurements and phase analysis using x-ray diffraction.

To obtain a ferrofluid, the gel-like product was centrifuged and washed to remove methanol, and then redispersed in deionized water. An aqueous solution of L-ascorbic acid (1 mM) was added to this suspension and the resulting mixture was stirred at room temperature for 24 hours, then sonicated for 30 minutes. It was purified by ultrafiltration through a 10,000 MWCO DIAFLO membrane at a nitrogen gas pressure of 60 psi. This resulted in a homogeneous suspension (ferrofluid) of iron oxide stabilized by HA. This ferrofluid had a solid content of 6.6 milligrams dry solid per milliliter of suspension and an iron (Fe) content of 40% w/w of dry solids as determined by elemental analysis.

Size analysis of this ferrofluid was done by TEM and QELS. TEM samples were prepared by dispersing the ferrofluid in 2-propanol, and placing a drop of this suspension on a carbon coated TEM grid and letting it dry. For QELS, dilute suspensions of the ferrofluid were

prepared in deionized water. Capillary Electrophoresis (CE) was used to characterize the surface charge and electric mobility of the ferrofluid particles. Samples for CE were prepared by adding 5% (v/v) of the HA based ferrofluid and 5% (v/v) of a stock solution of caffeine (1 mg/ml) to a sodium phosphate buffer. Caffeine acts as a neutral marker and can be used for the calculation of electroosmotic flow. Experiments were conducted at room temperature in a pH range of 5.5 to 11 (1mM, 10 mM, and 25 mM phosphate buffer concentrations) and for applied voltages of 15 to 30 kV. As indicated previously, the electrophoretic mobility of the HA-iron oxides was approximately 3 x $10^{-8} m^2/V$ sec.

Alternatively, magnetic gels may be prepared by degassing a solution of $FeCl_2$ (0.2 M, 25 ml) in methanol/water (50/50 v/v) by bubbling nitrogen for 15 minutes. A solution of HA (25 ml of 10 g L^{-1}) in methanol/water (50/50) was added dropwise under vigorous stirring using a syringe fitted with a 16 G needle. Gelation occurred immediately. The mixture was stirred under nitrogen for 3 hours. It was centrifuged to separate the Fe^{2+}-loaded HA gel from the solution. The gel was washed with methanol/water 3 times to remove any excess Fe^{2+}. This washed gel was placed into a flask containing 25 ml of 0.5 M sodium hydroxide solution in methanol/water (50/50 v/v). The mixture was stirred at room temperature for 23 hours, followed by oxygen bubbling for 2 hours. A brown, magnetic gel was formed. It was isolated from the mixture by centrifugation and washed with methanol/water. The above procedure (loading) was repeated five times to obtain a magnetic HA gel sample. The HA gel became darker in color and more magnetic after each loading and oxidation. A dark brown gel was obtained after five loading cycles.

The gel isolated after five loading cycles (20 mg) was dispersed in 2 ml of 1.0 mM sodium phosphate buffer (pH = 6.93) in an ultrasonic bath. Another gel sample (10 mg) was dispersed in 1 ml of 1.0 mM sodium phosphate buffer (pH = 6.93) in an ultrasonic bath. An aqueous solution of L-ascorbic acid (1.0 mM, 1 ml) was added and the resulting mixture was sonicated for 30 minutes. It was purified by dialysis against water at room temperature. Both suspensions are believed to be useful as MR Imaging agents.

Characterization of the gels and fluid

Determination of Iron Content in HA-Iron Oxide Gel

Samples of the HA-iron oxide gels were rinsed twice with water and then freeze-dried. Three separate samples (7-8 mg) were weighed accurately and placed in three test tubes. Concentrated hydrochloric acid (2 ml) was added to dissolve the samples. The resulting solutions were filtered. The filtrate was transferred to a 10 ml flask and diluted to 10 ml with

deionized water. This solution was transferred to a 25 ml flask, into which were added sequentially an aqueous solution of NH_2OH,HCl (2.5 ml, 50 g L^{-1}) and 5 ml of an aqueous solution of o-phenanthroline (5 ml, 1.0 g L^{-1}). The mixture was diluted to 25 ml with 1.2 M sodium acetate buffer (1.2 M, pH = 3.5). The absorbance was measured at 510 nm. The data were converted to Fe content using a calibration curve established from solutions of known concentrations. Table 5 shows the iron content of the gels after two, three, four, and five consecutive loadings.

Table 5. Iron Content of HA-Iron Oxide Gels

Loading	Iron Content (% Fe)
2	10
3	14
4	16
5	17

Determination of the total carbohydrate content of HA-iron oxides

Aqueous phenol (0.05 ml, 80% w/w) was added to a suspension of HA-iron oxide (2 ml, 5 to 40 ug/ml). Concentrated sulfuric acid (5 ml) was added rapidly to the solution as close to the surface of the liquid as possible. The solution was kept at room temperature for 10 minutes. It was then shaken and placed in a water bath kept at 30°C for 20 minutes. The absorbance of the solution at 490 nm was measured and carbohydrate content was calculated using a calibration curve obtained with HA solutions.

Assessment of the ability of the HA-based imaging agents to bind to human breast cancer cell lines

In order to determine the ability of HA-imaging agents to bind to human breast cancer cells, the fluorescent dye Cy3, Texas red, or any other suitable dye is coupled to HA-imaging agents complexed with liposomes. Binding studies include Cy3-HA alone to determine whether coupling with MR imaging agents alters binding to the cell surface. It is believed that HA-imaging agents complexed with liposomes may have a longer duration in cells because of the encapsulation in the liposomes. Cy3-HA is prepared with a procedure identical to that for preparing fluorescein isothiocyanate fluorochrome that emits at 590 nm with HA (FITC-HA), which has been used extensively for studying HA/cell surface interactions. Labeling of HA with Cy3 should not affect the binding properties of the HA. Cy3 is superior to FITC, because it does not rapidly fade.

The cell lines described in FIG. 1 are used for this study because their expression of HA receptors has been well described. Cells are prepared for flow cytometry (FACS) analysis, then incubated for 1 hour on ice with Cy3-HA imaging agents. Live cells are released from the substratum, incubated with FITC ILA± antibody, washed with phosphate buffered saline (PBS), and then cell surface fluorescence analyzed with the flow cytometer at a wavelength of 590 nm. To determine the specificity of binding, several approaches are used: a) cells are incubated with Cy3-HA-based imaging agents in the presence of a 100-fold excess of unlabeled HA and b) cells are incubated with Cy3-HA-based imaging agents that have been treated with streptomyces hyaluronidase to degrade the HA so that it does not bind to the receptors. Finally, the presence of HA receptors on cell surfaces of the cell lines described in Table 1 are confirmed with FACS analysis with monoclonal antibodies to RHAMM and CD44 that are available commercially (Applied Bioligand, Man, Can). Collectively, it is believed that these experiments will demonstrate that HA-imaging agents bind specifically to the cell surface as does Cy3-HA. Because the cell lines display varying levels of HA receptors, the results of these experiments should demonstrate a correlation between HA receptor display and the amount of Cy3-HA imaging agents bound.

Assessment of the ability of HA-based imaging agents to target human breast tumors in nude rats

It is expected that, of breast cancer cell lines which bind specifically to HA-based imaging agents, the cell line that binds the most strongly and the one that binds the most weakly to HA-based imaging agents will confirm the role of either or both the RHAMM and CD44 receptors. The ability of selected HA-imaging agents to target to these cell lines which were grown as xenografts in nude rats is determined. It was confirmed that these cells express CD44 and RHAMM in vivo by a procedure in which human breast cancer cells (10^6) are injected subcutaneously into nude rats and allowed to grow to a palpable tumor size. The tumor is excised and analyzed for cell surface display of RHAMM and CD44 by obtaining single cells and the cell surface binding of RHAMM and CD44 antibodies is quantified with FACS. For confirmation, protein lysates are prepared and the presence of RHAMM and CD44 is also detected in Western Blot assays. Further, mRNA is obtained from tumor cells and RT-PCR analysis of both RHAMM and CD44 is conducted, using appropriate primers.

The chosen cell lines (10^6 cells/rat) are then injected and tumors allowed to grow for varying periods of time in order to obtain tumors of increasing size. The HA-based imaging agents chosen from the above studies are then labeled with ^{125}I, so that the targeting ability can

be confirmed using phosphoimaging. All animals are imaged with MR, because this method may be more sensitive than phosphoimaging. For the experiments, animals are initially injected with 10 mg kg^{-1} of chondroitin sulfate to down-regulate scavenger receptors that take up HA in the liver. The double-labeled HA imaging agents are then injected intravenously one hour later, phosphoimaged, and the animals taken for MR imaging. Timing should not be a problem because studies indicate that HA targets tumors for 12-24 hours. It is believed that these experiments will show that HA-imaging agents can target human breast tumors and that they will demonstrate the smallest size of tumor that can be imaged using MR imaging.

Role of CD44 and RHAMM in targeting HA-imaging agents

It is expected that the role for CD44, RHAMM, or both in targeting can be directly demonstrated by several approaches. In the first approach, antibodies that have previously been shown to block the binding of FITC-HA on human myeloma cells are used. Prior to the use of antibodies in vivo, the ability of these antibodies to inhibit binding to Cy3-HA is detected using FACS analysis. The effect of antibodies on targeting of HA-imaging agents is attempted in vitro and then in vivo, ultimately using MR imaging. However, to delineate experimentally the optimum concentration of receptor antibody, the ability of these reagents to block targeting is initially assessed. Antibodies are injected into animals intravenously, one hour after the intravenous injection of chondroitin sulfate, and 0 to 15 minutes prior to injection of the HA.

It is believed that the effect on targeting can be quantified at varying times after injection. Binding of HA to its receptors is a complex event and it is possible that the antibodies that affect HA binding to myeloma cells do not affect HA binding to breast cancer cells. If these antibodies are not effective at blocking HA binding in vitro, anti-sense peptides to the HA binding domains of CD44 and RHAMM are used. This approach has been used successfully in vivo to block the AT-1 receptor. Both CD44 and RHAMM require the presence of a basic amino-acid motif to bind to HA, and anti-sense peptides to this region are prepared. They are administered in vitro or in vivo, as described above for antibodies. The effect of peptides on the distribution of HA is assessed with FACS. An effective concentration range is determined experimentally.

As another approach, a human combinatorial phage display library can be used to isolate antibodies that recognize the HA binding motifs of CD44 and of RHAMM, which are conserved in mouse to human. The attainment of monoclonal and polyclonal antibodies to these sequences has been attempted and it failed to raise a polyclonal response. However, use of the phage library allows the attainment of human antibodies that recognize these domains.

The recovery of these human antibodies allows for their use to test their effect on HA binding. Specifically, these antibodies may bind to the CD44 and RHAMM receptors and prevent HA or HA-based contrast agents from binding to them. Thus, the antibodies can clarify the role of CD44 and RHAMM in binding HA in cells.

Role of HA-Gd Contrast Agents in Central Nervous System (CNS) Disorders

Three examples of the use of HA-Gd contrast agents for CNS disorders include imaging of brain tumors, stroke-induced injury, and Alzheimer's type neural degeneration. Gadolinium is currently used to image CNS tumors, but is only effective at locations where there is breach of the blood-brain barrier making this procedure less effective in visualizing the entire tumor encompassing intact vascular areas. In Alzheimer's disease, current MR imaging can visualize only gross tissue atrophy which is only useful late in disease progression. In the case of stroke, compromised tissue can be visualized by MR. Nevertheless, this does not reveal the full extent of the vascular system that undergoes biomechanical changes that could contribute to further damage via secondary processes, such as those mediated by vascular invasion of inflammatory cells.

In each of the above conditions, there is evidence of upregulation of hyaluronan (HA) receptors either in neural tissue or associated blood vessels. These receptors include the HA receptors, RHAMM and CD44. Levels of intracellular adhesion molecule (ICAM-1) are also elevated in these conditions and ICAM appears to be identical to liver endothelial HA receptor which has been shown to bind to HA.

It is believed that the HA/gadolinium conjugate will allow MR imaging of not only CNS tissue where gadolinium is currently useful, but also areas where the blood brain barrier is intact and exhibits increased HA receptors, which is indicative of alterations in vascular and tissue functions that reflect potential local damage. This utility is based on evidence of an association between elevated HA receptors and tissue injury.

While various specific embodiments of the present invention have been described, modifications and substitutions may be made by those skilled in the art without departing from the true spirit and scope of the present invention. Accordingly, any modified or substituted variants of the present invention should be understood to fall within the scope of the appended claims in as much as the invention has been described by way of illustration only and not limitation.

What is Claimed:

1. An HA-based imaging agent comprising hyaluronan and gadolinium.

2. An HA-based imaging agent comprising hyaluronan, gadolinium, and liposomes.

3. An HA-based imaging agent comprising hyaluronan and an iron oxide.

4. The HA-based imaging agent of claim 1 further comprising diethylenetriamine pentaacetic acid.

5. The HA-based imaging agent of claim 4 wherein the imaging agent comprises about 3 to about 12 percent by weight of gadolinium.

6. The HA-based imaging agent of claim 4 wherein the imaging agent comprises about 5.6 to about 9.6 percent by weight of gadolinium.

7. The HA-based imaging agent of claim 6 wherein the average molecular weight of the hyaluronan is between about 20,000 and about 200,000.

8. The HA-based imaging agent of claim 6 wherein the average molecular weight of the hyaluronan is between about 50,000 and about 100,000.

9. A method of producing an HA-Gd imaging agent comprising the steps of:

combining hyaluronan having a carboxyl group with ethylenediamine to form an NH_2-modified hyaluronan;

contacting the NH_2-modified hyaluronan with diethylenetriamine pentaacetic acid to form a DTPA-modified hyaluronan; and

contacting the DTPA-modified hyaluronan with gadolinium to form an HA-gadolinium imaging agent.

10. A method of producing an HA-Gd imaging agent comprising the steps of:

combining hyaluronan having a carboxyl group with water to form an HA solution;

adding hydrochloric acid to the HA solution to adjust the pH of the HA solution to about 3.0;

adding 2-ethoxy-1-ethoxycarbonyl-1,2-dihydroquinoline in a methanol solution to the HA solution;

contacting the HA solution with ethylenediamine;

dialyzing the HA solution with a solution of an alcohol and water;

dialyzing the HA solution with water;

concentrating and freeze-drying the HA solution to form an NH_2-modified hyaluronan;

adding triethylamine to a solution of diethylenetriamine pentaacetic acid in acetonitrile to form a DTPA solution

contacting the NH_2-modified hyaluronan with the DTPA solution to form a HA-DTPA solution;

maintaining the pH of the HA-DTPA solution at about 10.0;

freeze-drying the HA-DTPA solution to form a DTPA-modified hyaluronan;

contacting the DTPA-modified hyaluronan with a solution of gadolinium chloride in water to form a HA-DTPA-Gd solution; and

freeze-drying the HA-DTPA-Gd solution to form an HA-gadolinium imaging agent.

11. A method of making an HA-iron oxide imaging agent comprising:

contacting hyaluronan with iron chloride to form a gel;

removing uncomplexed iron ions from the gel;

treating the gel with hydroxide; and

bubbling the gel with oxygen to form a magnetic gel.

12. A method of determining whether a tumor cell is benign or malignant by measuring the presence or absence of an HA receptor, comprising:

contacting a tumor cell with an hyaluronan-based imaging agent and an imaging agent having no hyaluronan;

comparing the signals generated by the imaging agents to determine the presence or absence of an HA receptor; and

evaluating whether a tumor cell is benign or malignant from the presence or absence of an HA receptor.

13. A method of testing binding of HA-based imaging agents to a cell line comprising:

labeling an HA-based imaging agent with a fluorescent dye to form a labeled imaging agent;

adding a group of cells from a cell line to the labeled imaging agent to generate a signal; and

determining cell binding from the signal.

14. A method of imaging an animal with an HA-based imaging agent comprising:

administering chondroitin sulfate to the animal;

administering an HA-based imaging agent to the animal; and

imaging the animal.

15. The method of claim 14 wherein the animal is human and the HA-based imaging agent comprises hyaluronan and gadolinium.

16. The method of claim 15 wherein the HA-based imaging agent further comprises diethylenetriamine pentaacetic acid.

17. The method of claim 16 wherein the imaging is done by magnetic resonance imaging.

Characteristics of human breast cancer cell lines

	Nude mouse[a]				In vitro					
Cell line	ER	Tumor.	Inv.	Met.	BCC Inv.[b]	CD44[c]	Motility[d]	Inv[e]	HA[f]	RHAMM[g]
MDA-MB-231	-	+	+	+	+++++	+++	21.30±1.11	+	23.38±2.16	5.855
MCF-7	+	+	-	-	++	+	13.39±0.84	-	7.13±1.67	4.049
MDA-MB-468	-	+	-	-	+	++++	5.91±0.23	-	3.85±0.89	2.948
R-75-1	+	+	-	-	+	-	7.47±0.22	-	6.73±1.16	2.205
1-47-D	+	-	-	-	-	-	6.54±0.27	-	2.54±0.74	0.964
S-578-T	-	+	+	+	+++++	+++++	4.43±0.27	++	280.0± 20.0	3.174

a From Thomson et al. 1992 (56), Brünner et al. 1993 (57). Tumorigenesis, local invasion and metastasis in athymic nude mouse (NCr *nu/nu*).

b From Thomson et al. 1992 (56). Activity in Boyden chemaber chemoinvasion assay. Graded as % of the MDA-MB-231 activity (+ 0-20%, ++20-40%m ++++ 60-80%, +++++ >80%).

c From Culty et al. 1994 (23). CD44 content relative to HCV-29T cells, quantified by dot blot analysis with the BU52 mAb.

d Random locomotion measured by using a computerized timelapse image analysis system (μm/h).

e Invasion assess determined by the cells entered collagen gels *in vitro*.

f HA production ($\mu g/L/10^6$ cells).

g RHAMM expression, OD value from densitometric analysis of Western blots.

FIG. 1

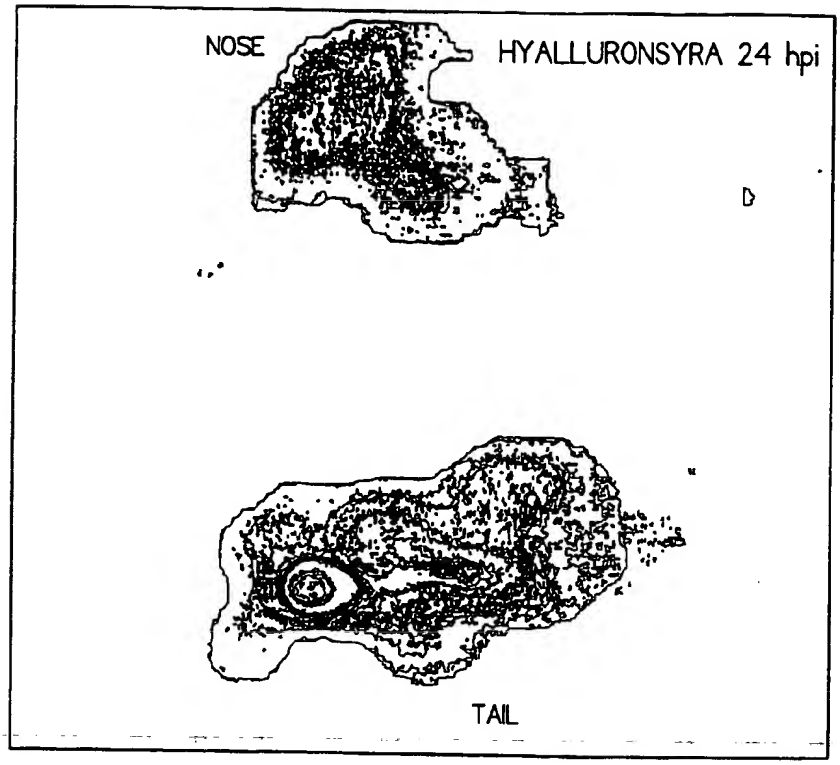

FIG. 2

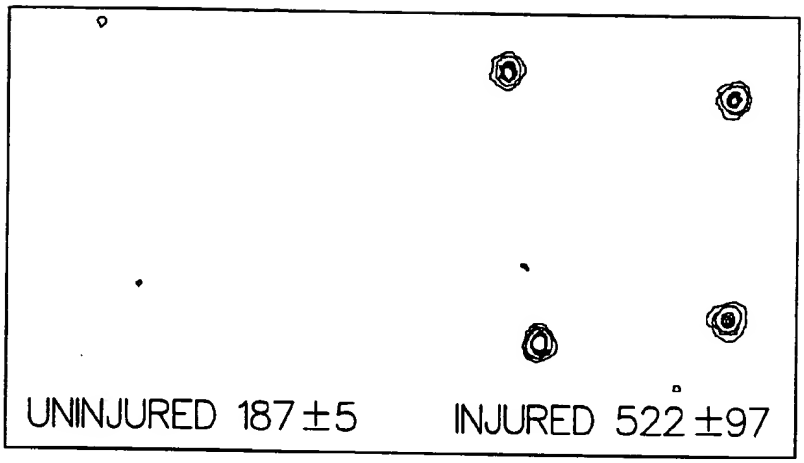

FIG. 3

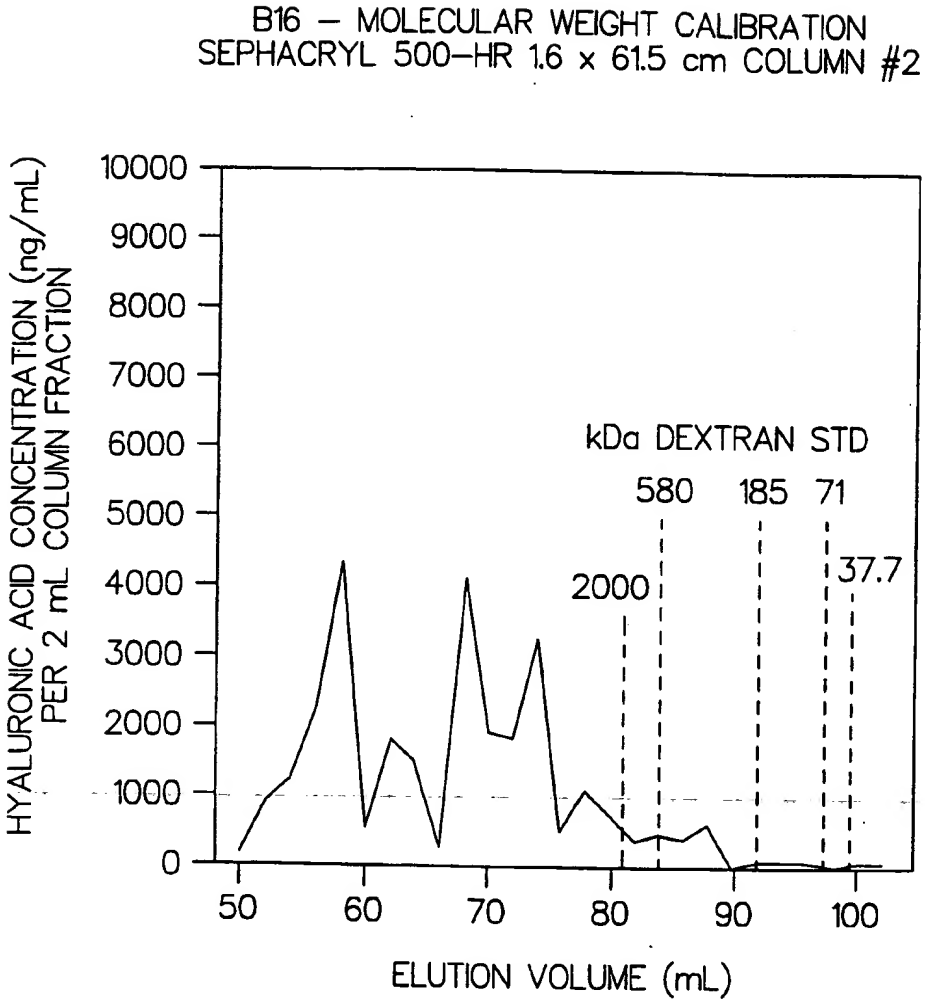
B16 – MOLECULAR WEIGHT CALIBRATION
SEPHACRYL 500–HR 1.6 x 61.5 cm COLUMN #2
HYALURONIC ACID CONCENTRATION (ng/mL)
PER 2 mL COLUMN FRACTION
10000
9000
8000
7000
6000
5000
4000
3000
2000
1000
0
kDa DEXTRAN STD
580
185
71
37.7
2000
50
60
70
80
90
100
ELUTION VOLUME (mL)

FIG. 4

FIG. 5

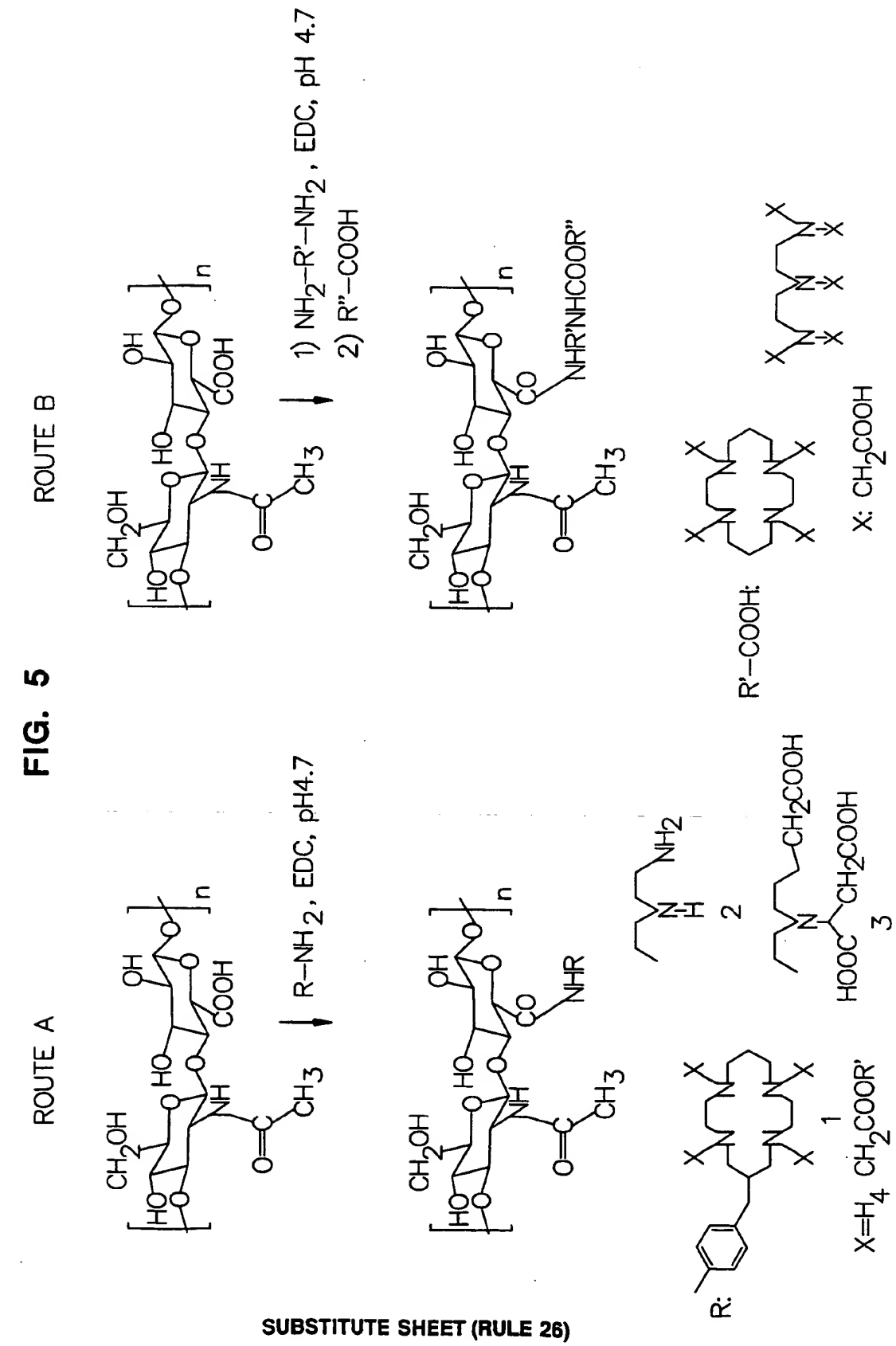
ROUTE A
ROUTE B
1) NH_2–R'–NH_2, EDC, pH 4.7
2) R"–COOH
R–NH_2, EDC, pH4.7
R'–COOH:
X: CH_2COOH
X=H_4 CH_2COOR'
R:
1
2
3
HOOC
CH_2COOH
CH_2COOH
NHR'NHCOOR"
NHR
NH_2

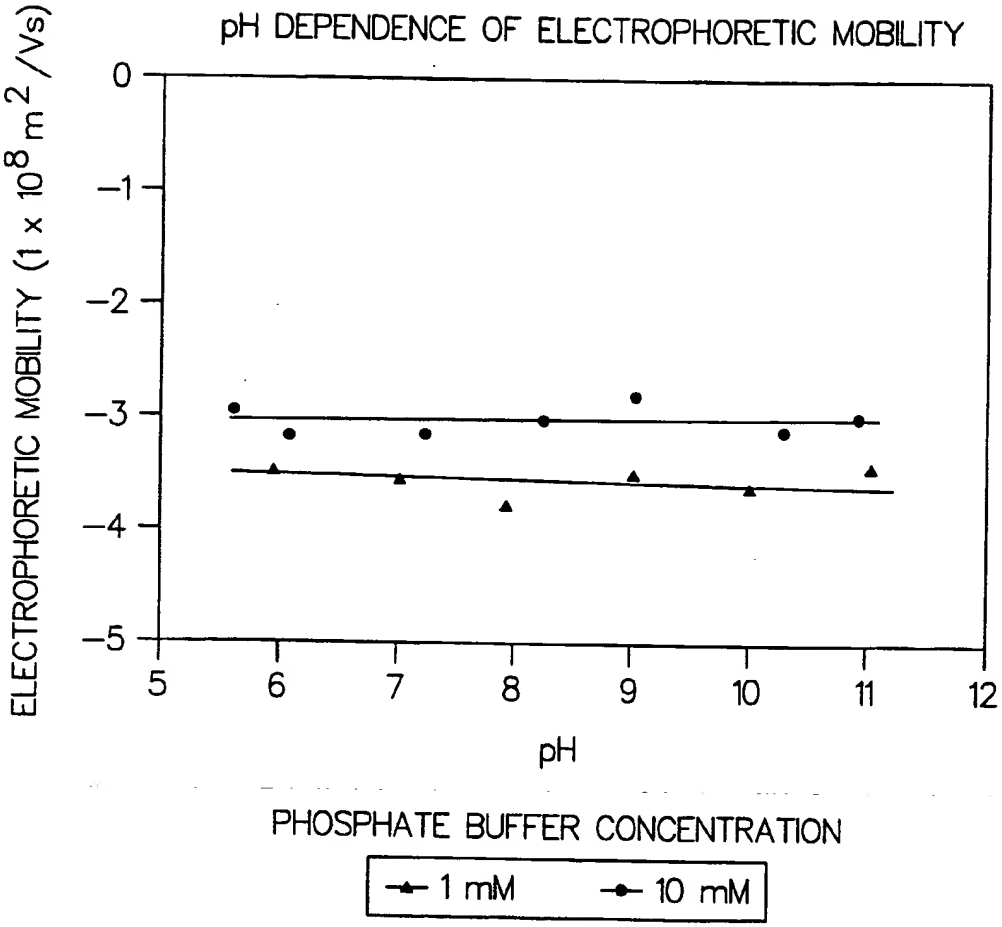
pH DEPENDENCE OF ELECTROPHORETIC MOBILITY
ELECTROPHORETIC MOBILITY (1 x 10^8 m^2/Vs)
0
−1
−2
−3
−4
−5
5
6
7
8
9
10
11
12
pH
PHOSPHATE BUFFER CONCENTRATION
1 mM
10 mM

FIG. 6

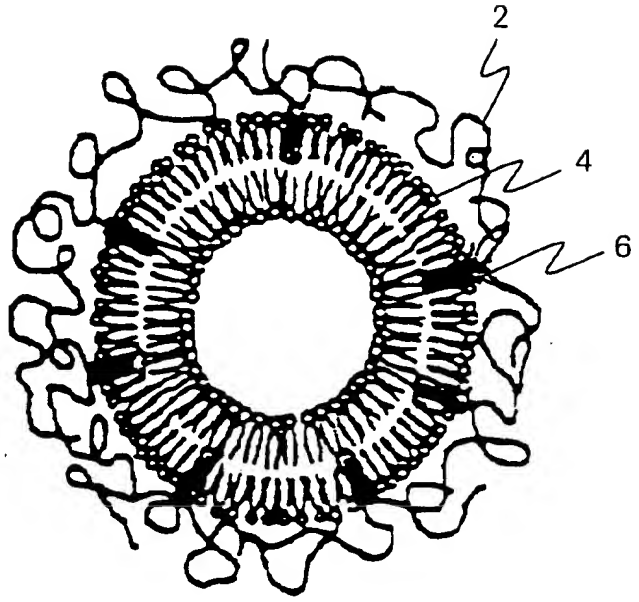

FIG. 7

FIG. 8

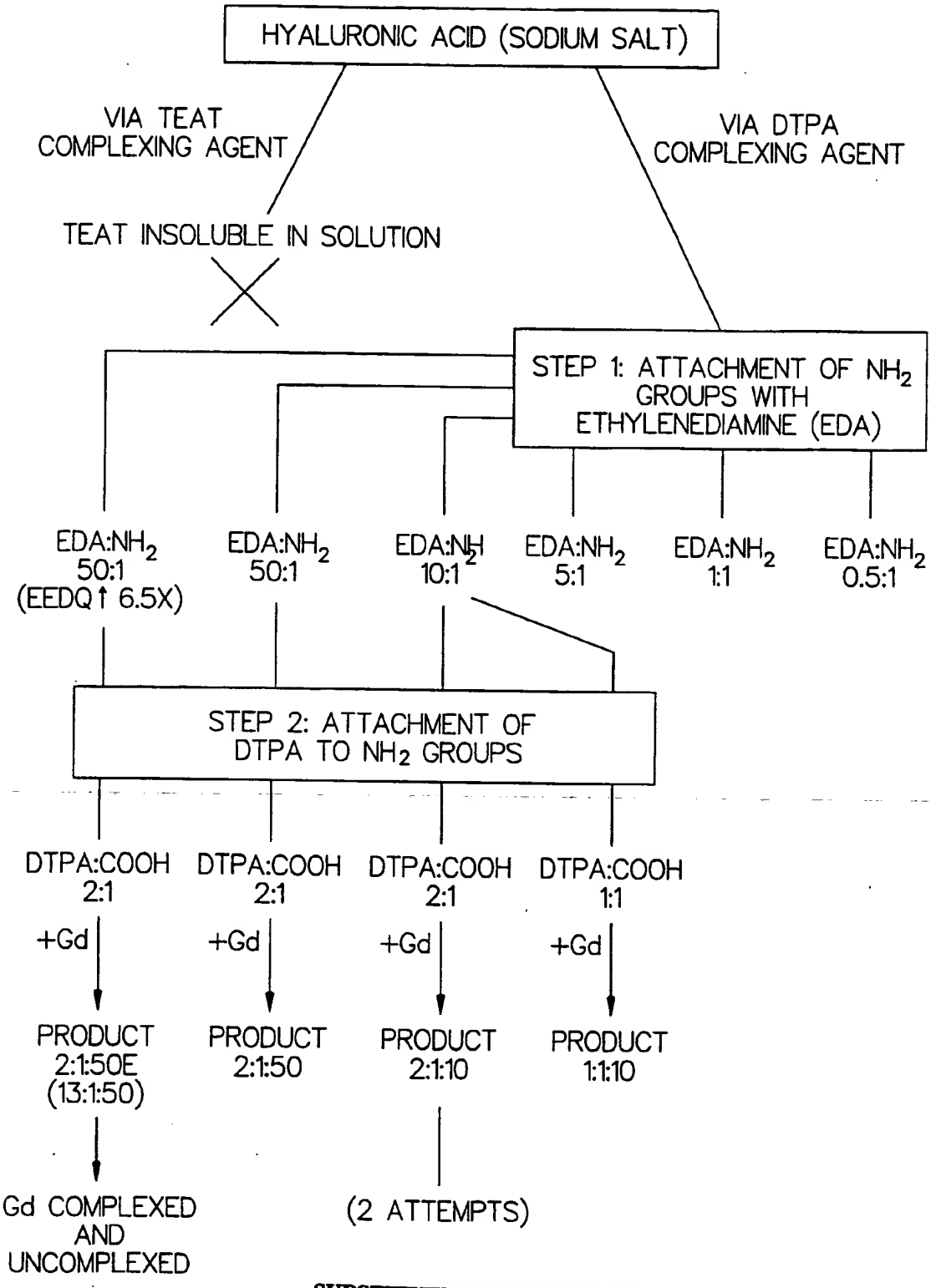
HYALURONIC ACID (SODIUM SALT)
VIA TEAT COMPLEXING AGENT
VIA DTPA COMPLEXING AGENT
TEAT INSOLUBLE IN SOLUTION
STEP 1: ATTACHMENT OF NH2 GROUPS WITH ETHYLENEDIAMINE (EDA)
EDA:NH2 50:1 (EEDQ ↑ 6.5X)
EDA:NH2 50:1
EDA:NH2 10:1
EDA:NH2 5:1
EDA:NH2 1:1
EDA:NH2 0.5:1
STEP 2: ATTACHMENT OF DTPA TO NH2 GROUPS
DTPA:COOH 2:1
DTPA:COOH 2:1
DTPA:COOH 2:1
DTPA:COOH 1:1
+Gd
+Gd
+Gd
+Gd
PRODUCT 2:1:50E (13:1:50)
PRODUCT 2:1:50
PRODUCT 2:1:10
PRODUCT 1:1:10
Gd COMPLEXED AND UNCOMPLEXED
(2 ATTEMPTS)

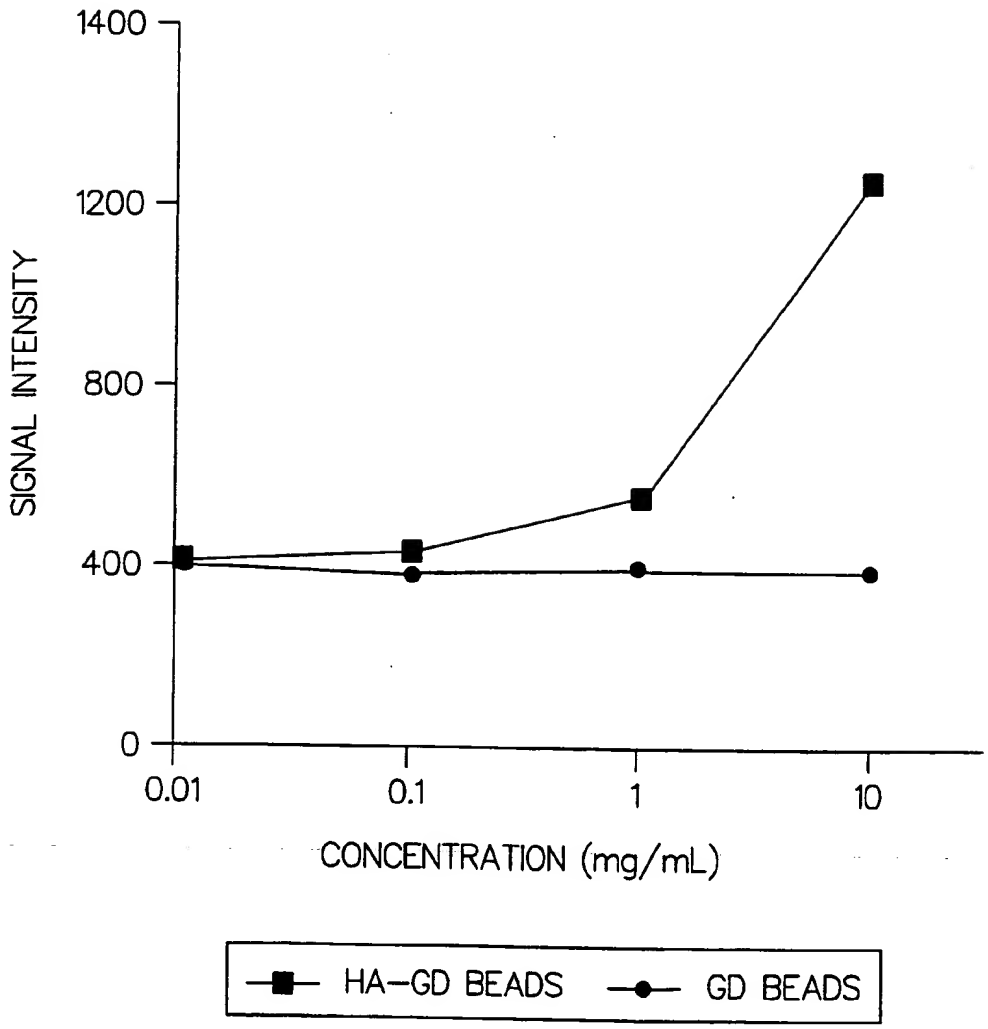
1400
1200
800
400
0
SIGNAL INTENSITY
0.01
0.1
1
10
CONCENTRATION (mg/mL)
HA-GD BEADS
GD BEADS

FIG. 9

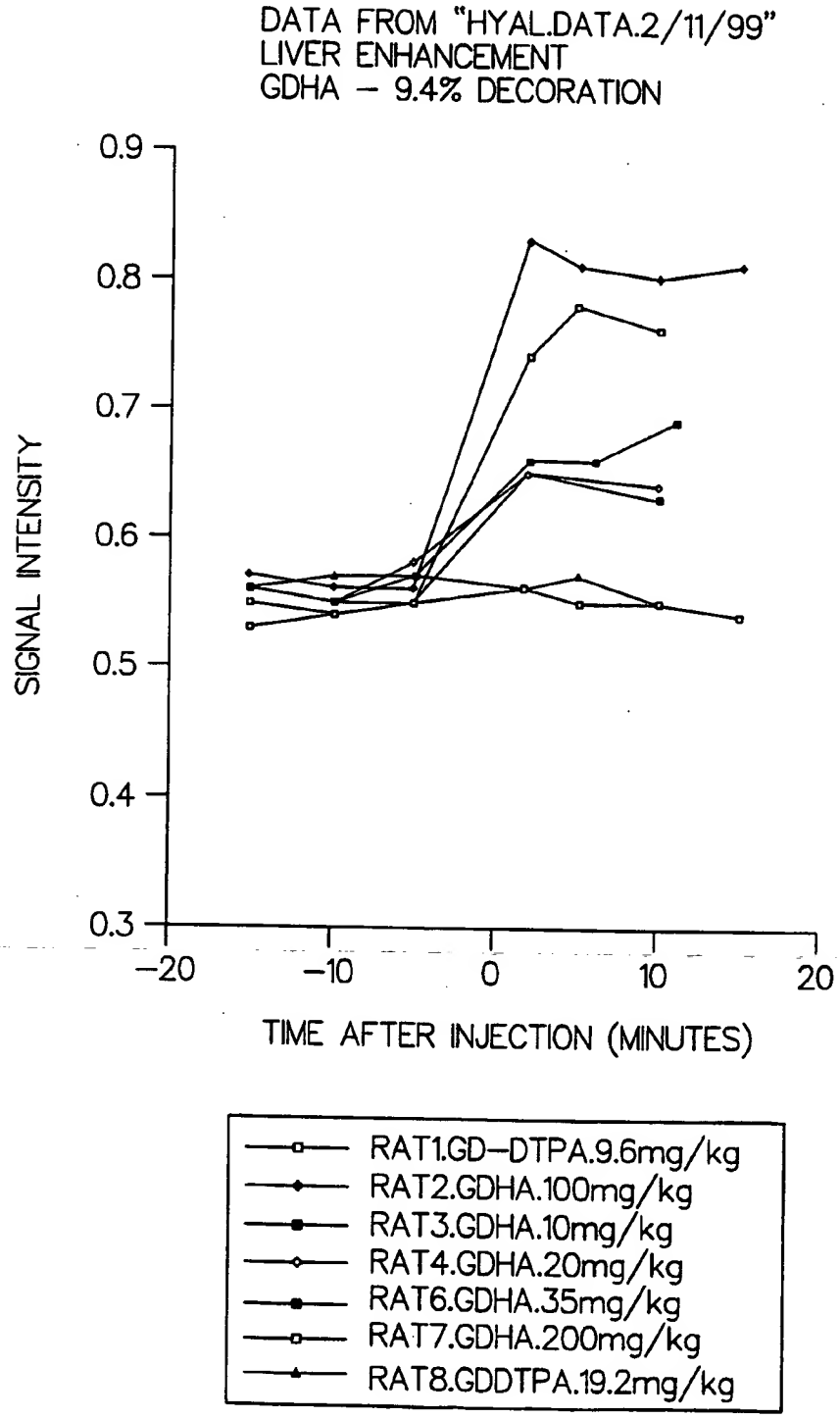
DATA FROM "HYAL.DATA.2/11/99"
LIVER ENHANCEMENT
GDHA – 9.4% DECORATION
SIGNAL INTENSITY
0.9
0.8
0.7
0.6
0.5
0.4
0.3
−20
−10
0
10
20
TIME AFTER INJECTION (MINUTES)
RAT1.GD–DTPA.9.6mg/kg
RAT2.GDHA.100mg/kg
RAT3.GDHA.10mg/kg
RAT4.GDHA.20mg/kg
RAT6.GDHA.35mg/kg
RAT7.GDHA.200mg/kg
RAT8.GDDTPA.19.2mg/kg

FIG. 10

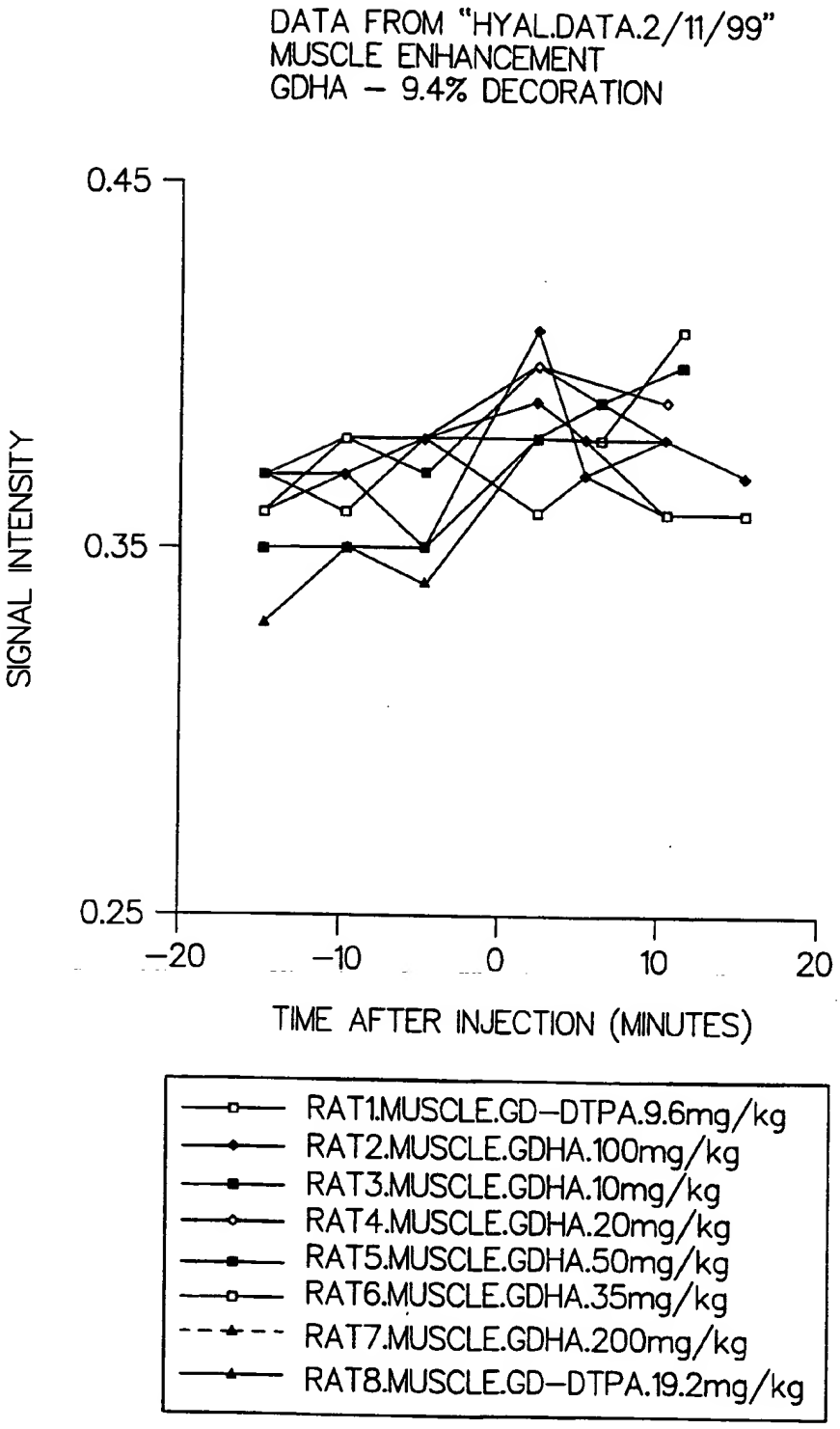
DATA FROM "HYAL.DATA.2/11/99"
MUSCLE ENHANCEMENT
GDHA – 9.4% DECORATION
0.45
0.35
0.25
SIGNAL INTENSITY
–20
–10
0
10
20
TIME AFTER INJECTION (MINUTES)
RAT1.MUSCLE.GD–DTPA.9.6mg/kg
RAT2.MUSCLE.GDHA.100mg/kg
RAT3.MUSCLE.GDHA.10mg/kg
RAT4.MUSCLE.GDHA.20mg/kg
RAT5.MUSCLE.GDHA.50mg/kg
RAT6.MUSCLE.GDHA.35mg/kg
RAT7.MUSCLE.GDHA.200mg/kg
RAT8.MUSCLE.GD–DTPA.19.2mg/kg

FIG. 11

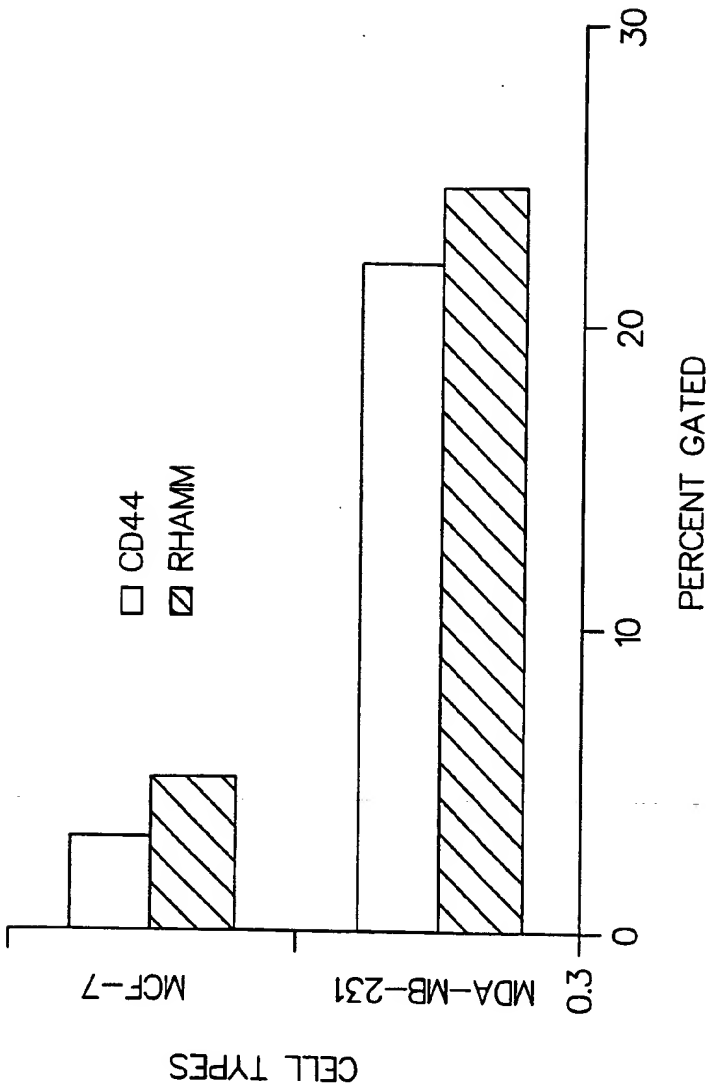
30
20
10
0
PERCENT GATED
CD44
RHAMM
MCF-7
MDA-MB-231
0.3
CELL TYPES

FIG. 12

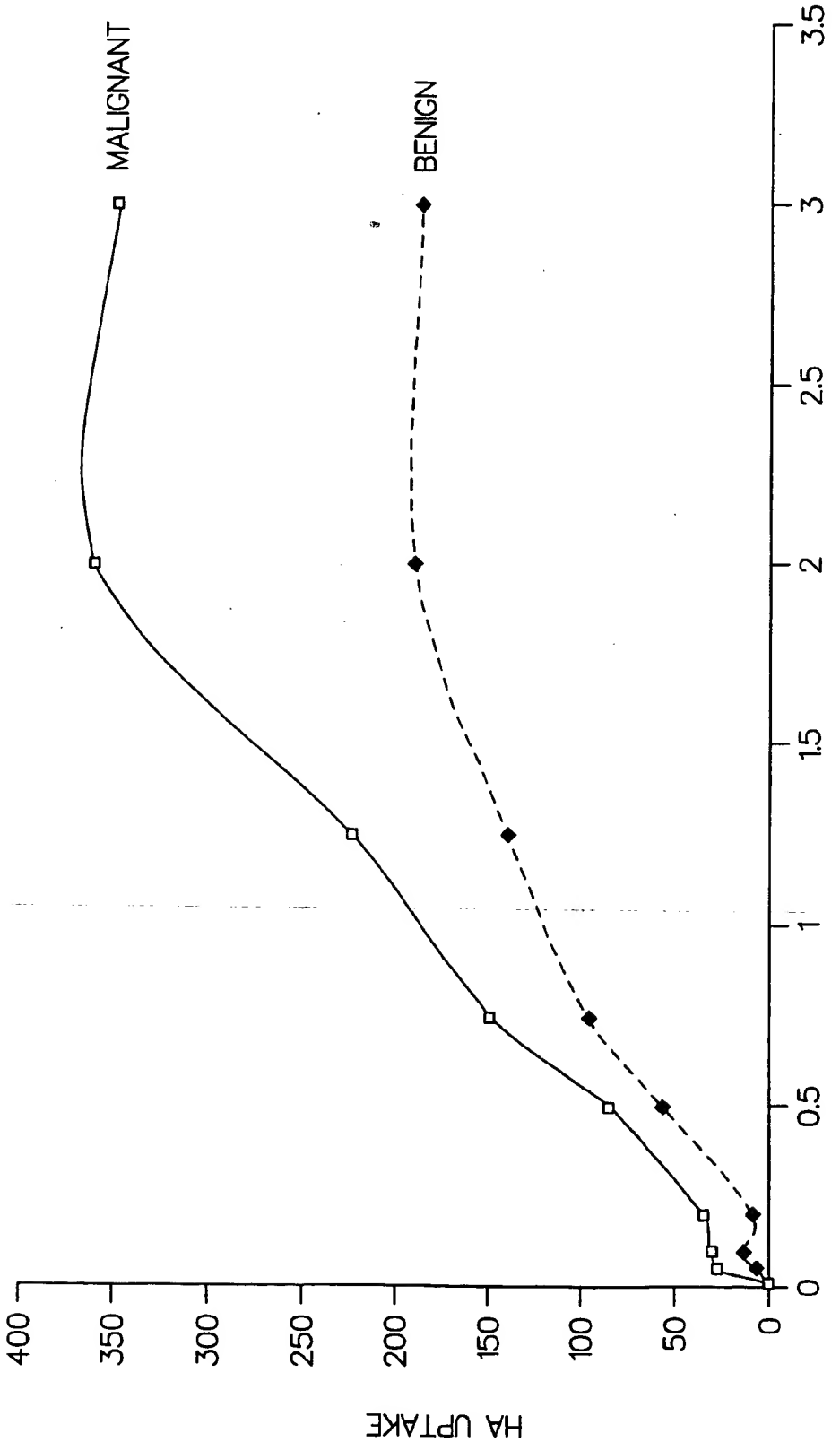
MALIGNANT
BENIGN
HA UPTAKE
400
350
300
250
200
150
100
50
0
0
0.5
1
1.5
2
2.5
3
3.5
HA CONCENTRATION (mg/mL)

FIG. 13

FIG. 14

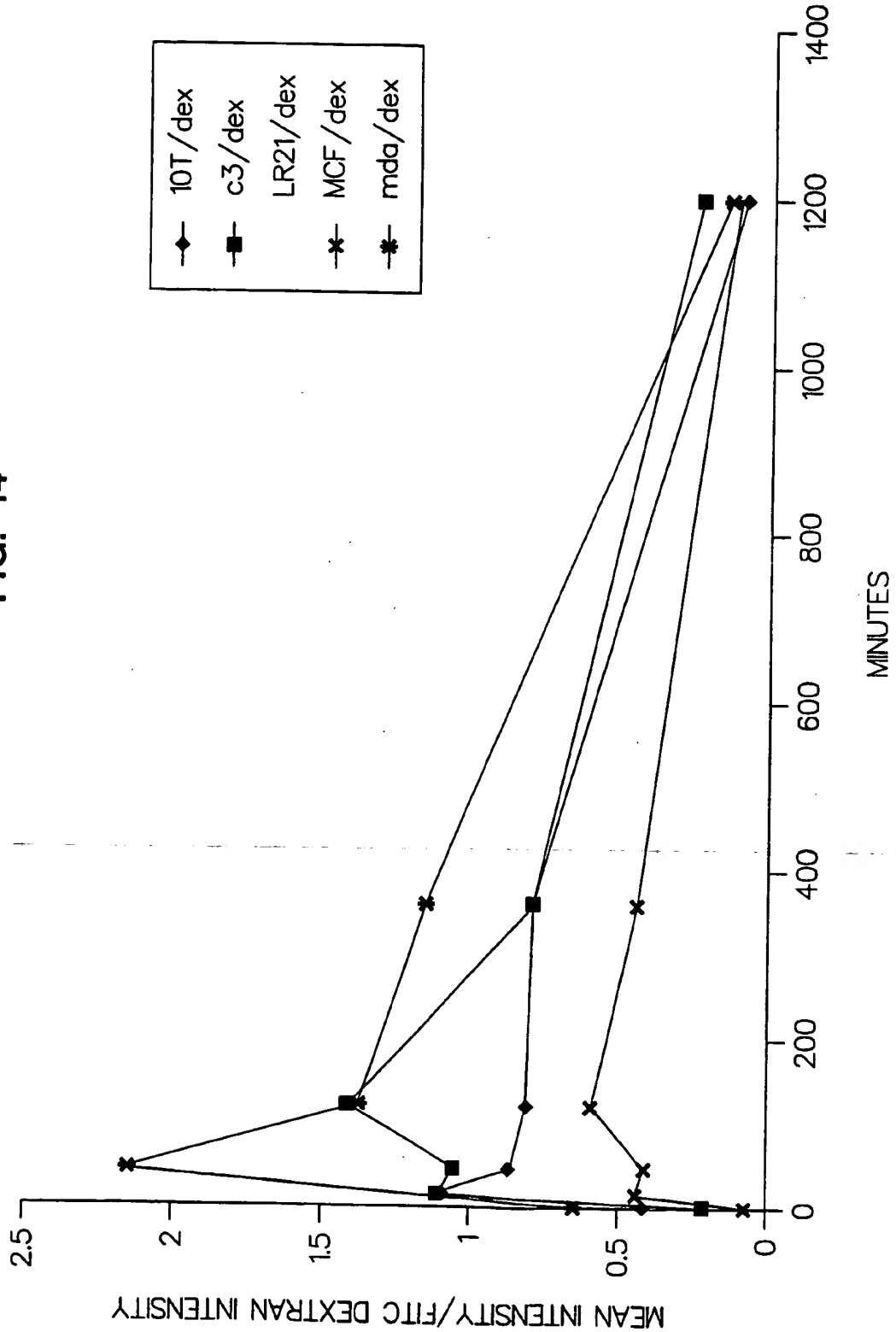
10T/dex
c3/dex
LR21/dex
MCF/dex
mda/dex
MEAN INTENSITY/FITC DEXTRAN INTENSITY
2.5
2
1.5
1
0.5
0
0
200
400
600
800
1000
1200
1400
MINUTES

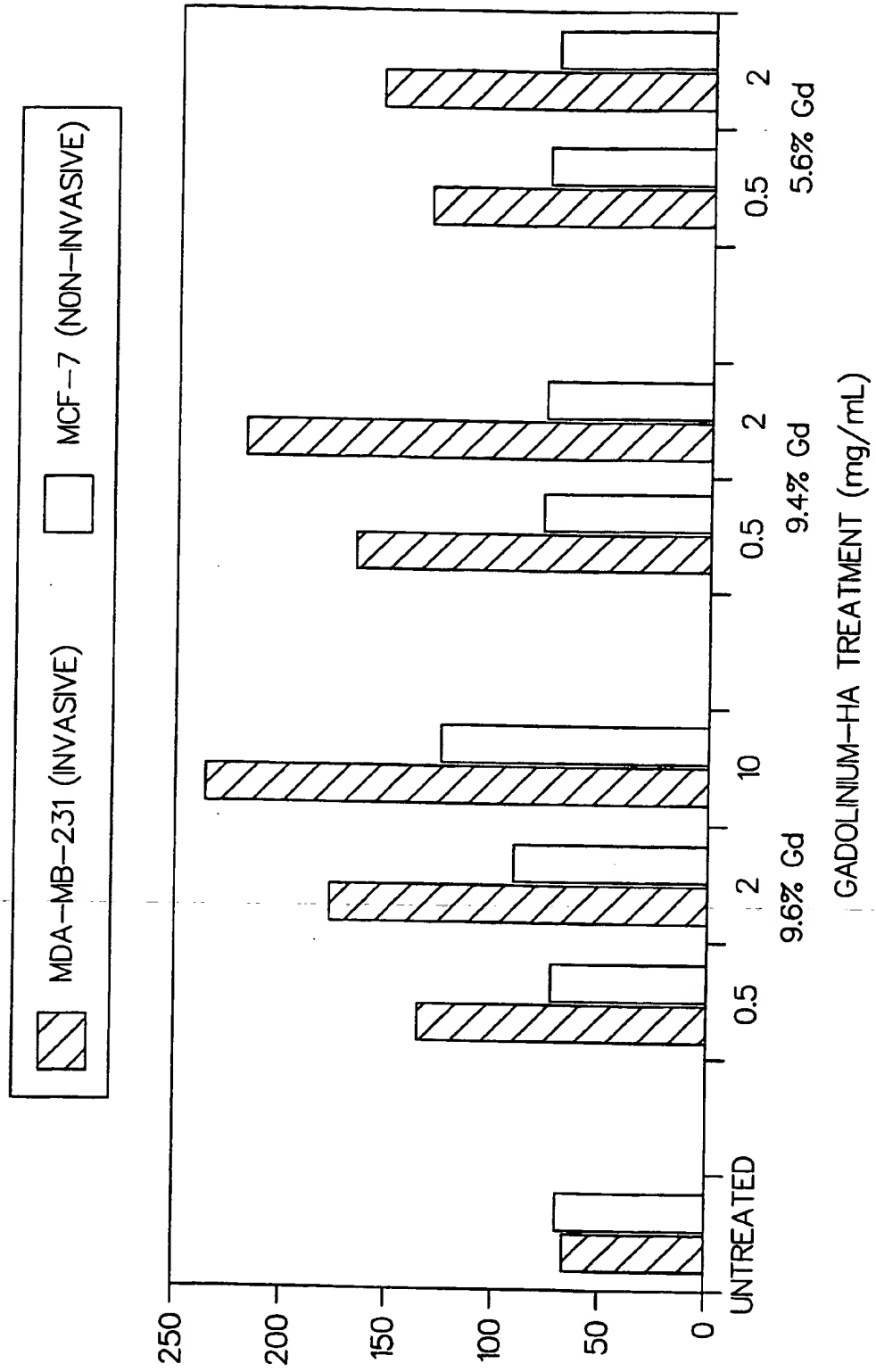
MDA-MB-231 (INVASIVE)
MCF-7 (NON-INVASIVE)
SIGNAL INTENSITY
250
200
150
100
50
0
UNTREATED
0.5
2
9.6% Gd
10
0.5
2
9.4% Gd
0.5
2
5.6% Gd
GADOLINIUM-HA TREATMENT (mg/mL)

FIG. 15

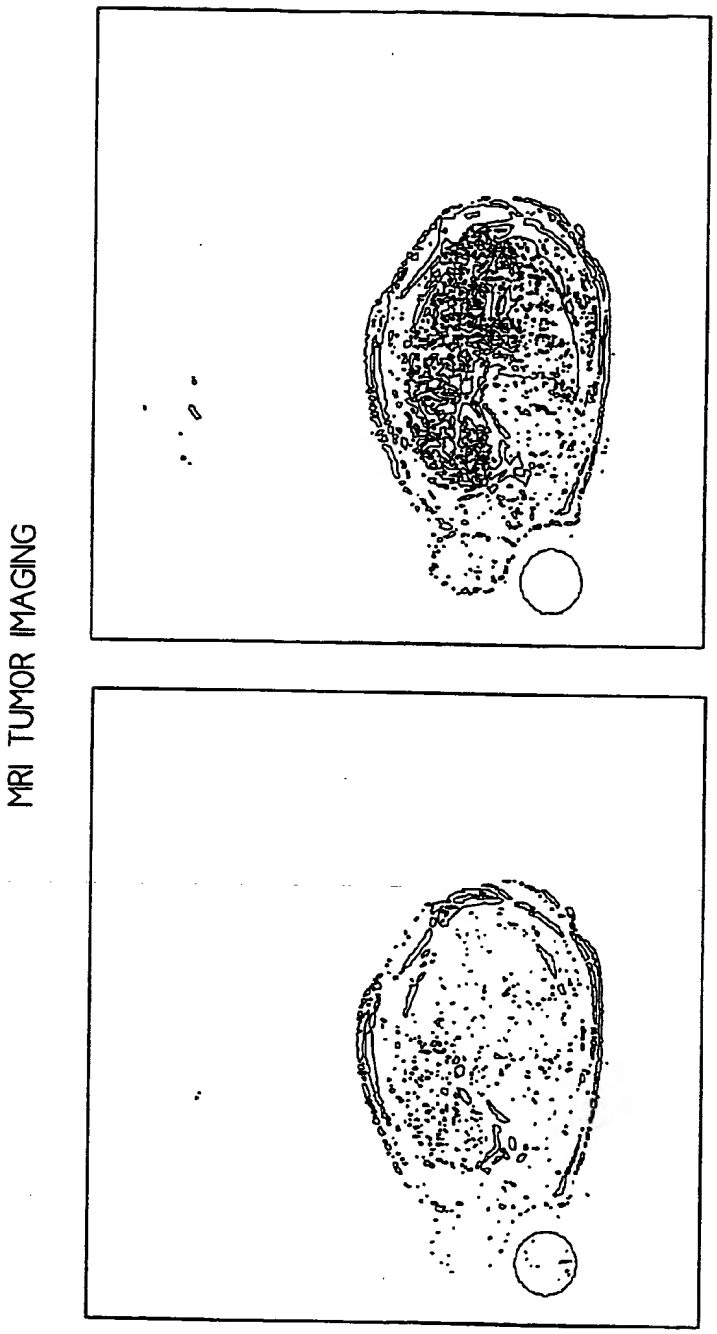

FIG. 16

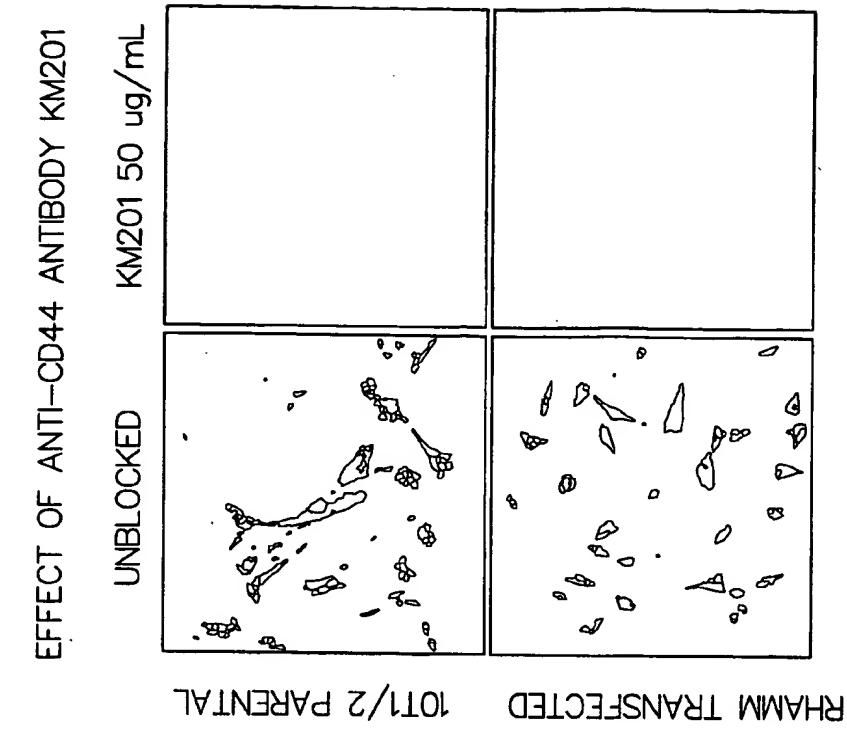
EFFECT OF ANTI-CD44 ANTIBODY KM201
UNBLOCKED
KM201 50 ug/mL
10T1/2 PARENTAL
RHAMM TRANSFECTED

FIG. 18

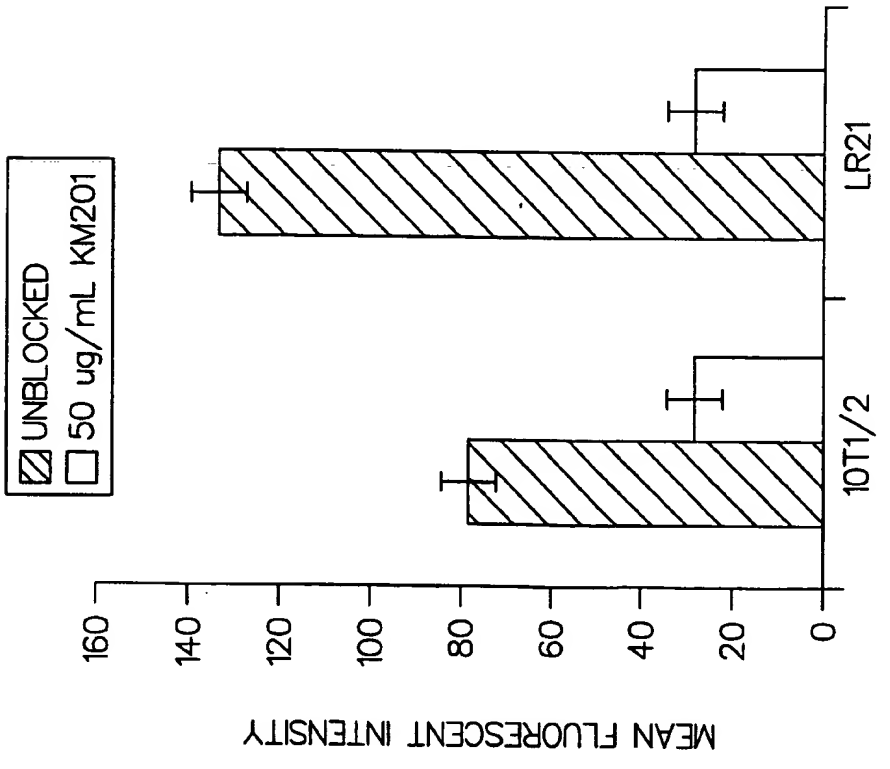
UNBLOCKED
50 ug/mL KM201
MEAN FLUORESCENT INTENSITY
160
140
120
100
80
60
40
20
0
10T1/2
LR21

FIG. 17

INTERNATIONAL SEARCH REPORT

International application No.
PCT/US99/09177

A. CLASSIFICATION OF SUBJECT MATTER

IPC(6) :A61B 5/055
US CL :424/9.35; 514/836; 600/420

According to International Patent Classification (IPC) or to both national classification and IPC

B. FIELDS SEARCHED

Minimum documentation searched (classification system followed by classification symbols)

U.S. : 424/9.35; 514/836; 600/420

Documentation searched other than minimum documentation to the extent that such documents are included in the fields searched

Electronic data base consulted during the international search (name of data base and, where practicable, search terms used)

CHEMICAL ABSTRACT (registry and text)
search terms: hyaluronic acid, MRI

C. DOCUMENTS CONSIDERED TO BE RELEVANT

Category*	Citation of document, with indication, where appropriate, of the relevant passages	Relevant to claim No.
X	US, 5,368,840 A (UNGER) 29 November 1994, col. 5, line 10, col. 6, line 5, lines 30-65, claims 9, 38, 65, 82, 87, and 93.	1-17
X	US, 5,593,658 A (BOGDANOV et al) 14 January 1997, col. 8, lines 54-64, col. 9, lines 29-56	1-17
Y	US, 5,707,604 A (RANNEY) 13 January 1998, col. 6, lines 12-22.	1-17
Y, P	US 5,756,069 A (TORCHILIN et al) 26 May 1998, col. 5, lines 2-30, col. 10, lines 21-28.	1-17
Y	US 5,449,508 A (UNGEr) 12 September 1995, col. 6, lines 46-66, col. 8, line 2.	1-17

☐ Further documents are listed in the continuation of Box C. ☐ See patent family annex.

*	Special categories of cited documents:	"T"	later document published after the international filing date or priority date and not in conflict with the application but cited to understand the principle or theory underlying the invention
"A"	document defining the general state of the art which is not considered to be of particular relevance	"X"	document of particular relevance; the claimed invention cannot be considered novel or cannot be considered to involve an inventive step when the document is taken alone
"E"	earlier document published on or after the international filing date	"Y"	document of particular relevance; the claimed invention cannot be considered to involve an inventive step when the document is combined with one or more other such documents, such combination being obvious to a person skilled in the art
"L"	document which may throw doubts on priority claim(s) or which is cited to establish the publication date of another citation or other special reason (as specified)	"&"	document member of the same patent family
"O"	document referring to an oral disclosure, use, exhibition or other means		
"P"	document published prior to the international filing date but later than the priority date claimed		

Date of the actual completion of the international search 16 JULY 1999	Date of mailing of the international search report 17 AUG 1999
Name and mailing address of the ISA/US Commissioner of Patents and Trademarks Box PCT Washington, D.C. 20231 Facsimile No. (703) 305-3230	Authorized officer GARY E. HOLLINDEN Telephone No. (703) 308-4521

Form PCT/ISA/210 (second sheet)(July 1992)*